HYDRAULICS OF SUBMERGED WALL-JETS AND RESULTING DOWNSTREAM SCOUR

Subhasish Dey, *Chair Professor*

Department of Civil Engineering
Indian Institute of Technology
Kharagpur, West Bengal
INDIA

Present study focused on

- Response of the turbulent flow field in submerged wall jets on horizontal beds to an abrupt changes in bed roughness (smooth bed followed by a rough bed)
- scour of non-cohesive sediment bed downstream of an apron
- development an analytical model of scour of sediment bed downstream of a smooth apron
- profile of the equilibrium scour hole
- time-variation of maximum scour depth
- effect of upward seepage on equilibrium scour hole and time-variation of maximum scour depth

Characteristics of Sediments Used in the Experiments

Median size d_{50}(mm)	Relative density s	Geometric standard deviation σ_g	Angle of repose ϕ (degree)
0.8	2.65	1.3	30
1.86	2.65	1.27	31.5
3	2.65	1.19	34

Submerged wall jets on rigid beds

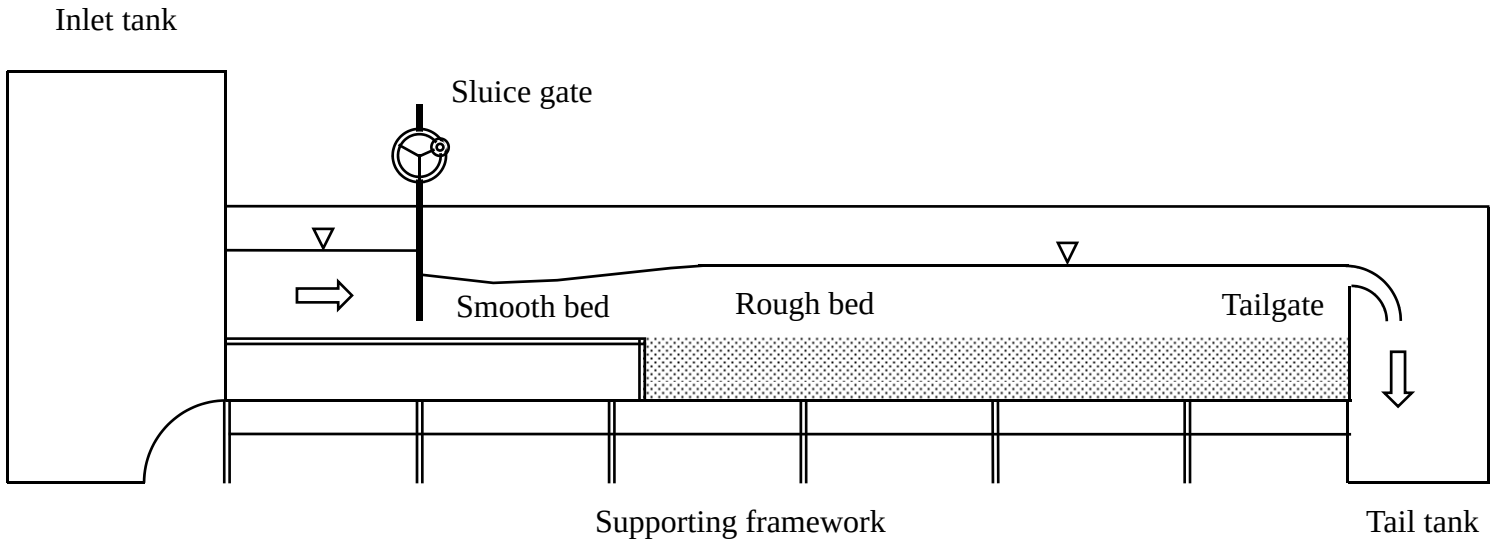

- **Sluice gate openings b = 10 mm, 12.5 mm and 15 mm**
- **Submergence factors = 0.96 to 1.85**
- **Jet Froude numbers = 2.58 to 4.87**
- **Issuing velocity of jet U = 0.99 – 1.525 m/s**
- **Tailwater depth = 0.114 – 0.163 m**
- **Length of apron = 0.4 and 0.5 m**

Flow Field in Submerged Wall Jets on Abrupt Changes of Bed Roughness

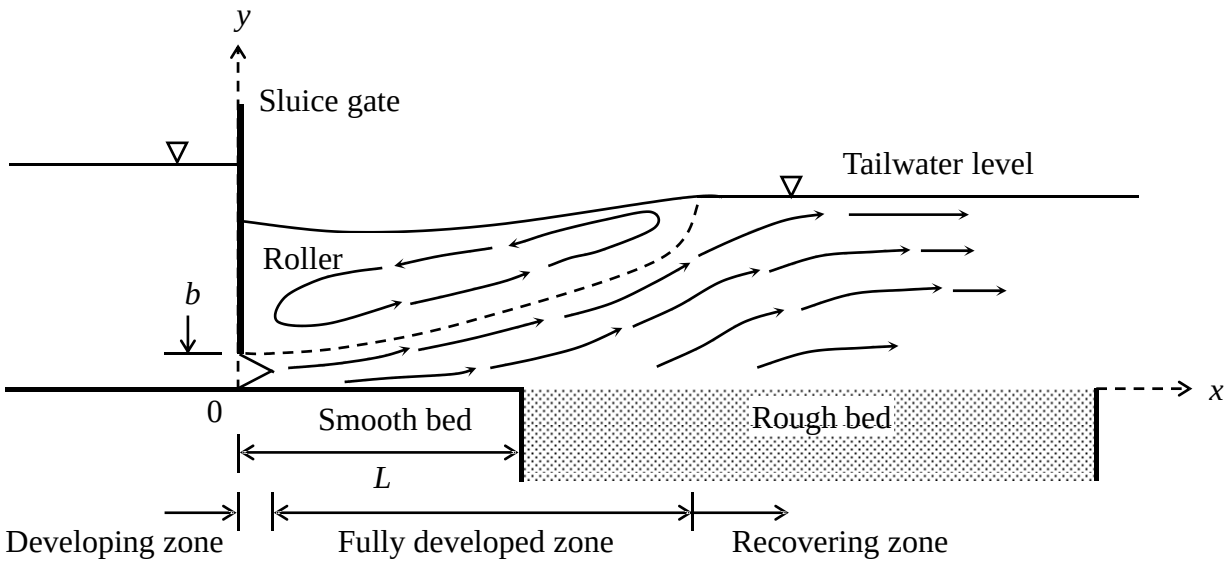

flow zones in a submerged wall jet

- submerged jet has three flow zones
- developing zone is the flow zone in the immediate vicinity of the issuing section of jet
- fully developed zone is the intermediate flow zone having a flow reversal
- recovering zone starts where the fully developed zone ends

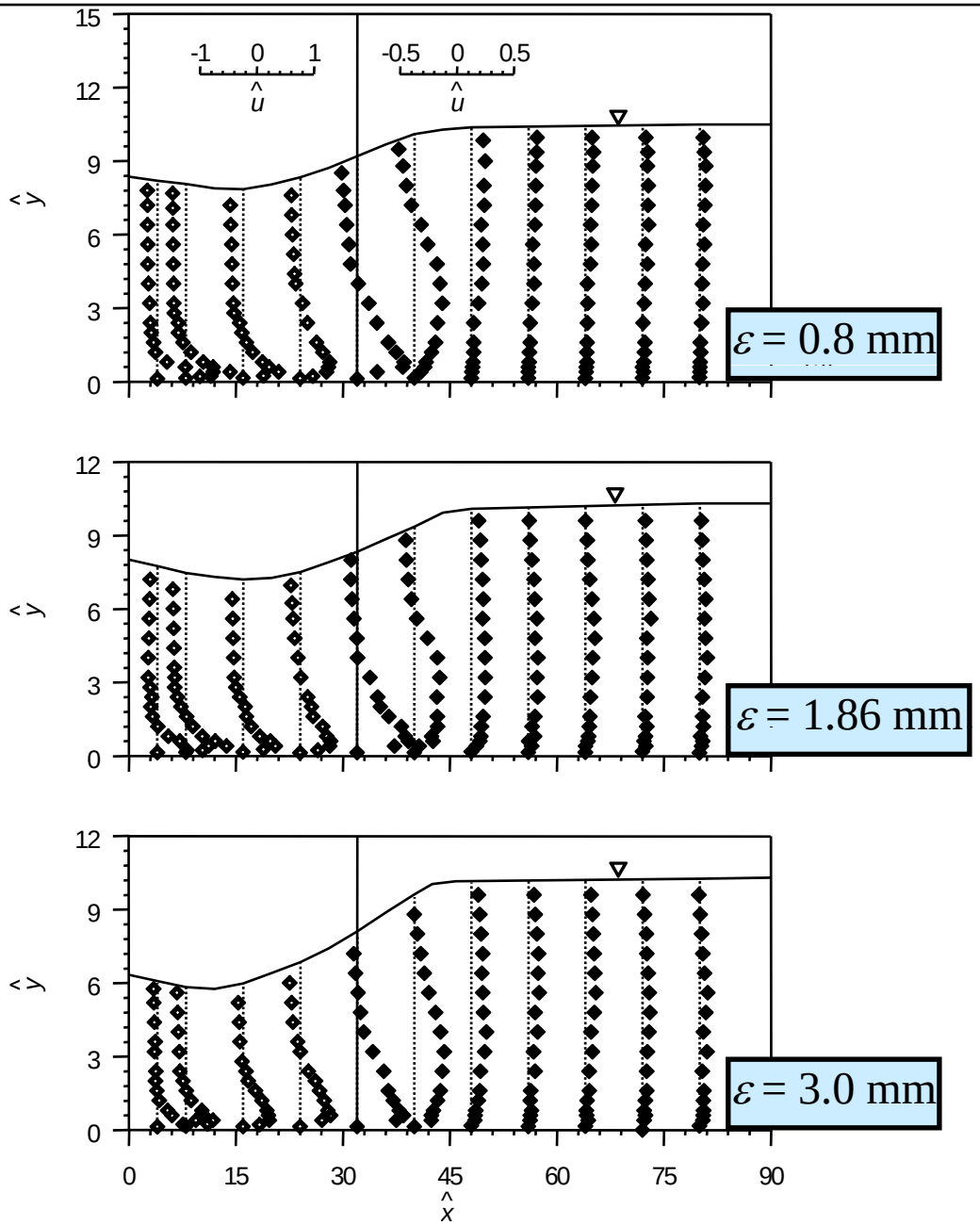

Vertical distributions of $\hat{u}$

- depression of free surface elevation and the variation of free surface curvature in the developing and fully developed zones
- reversal nature of u signifies an apparent swirl flow (surface roller), which is missing in the recovering zone
- growth of the boundary layer expedites with increase in roughness

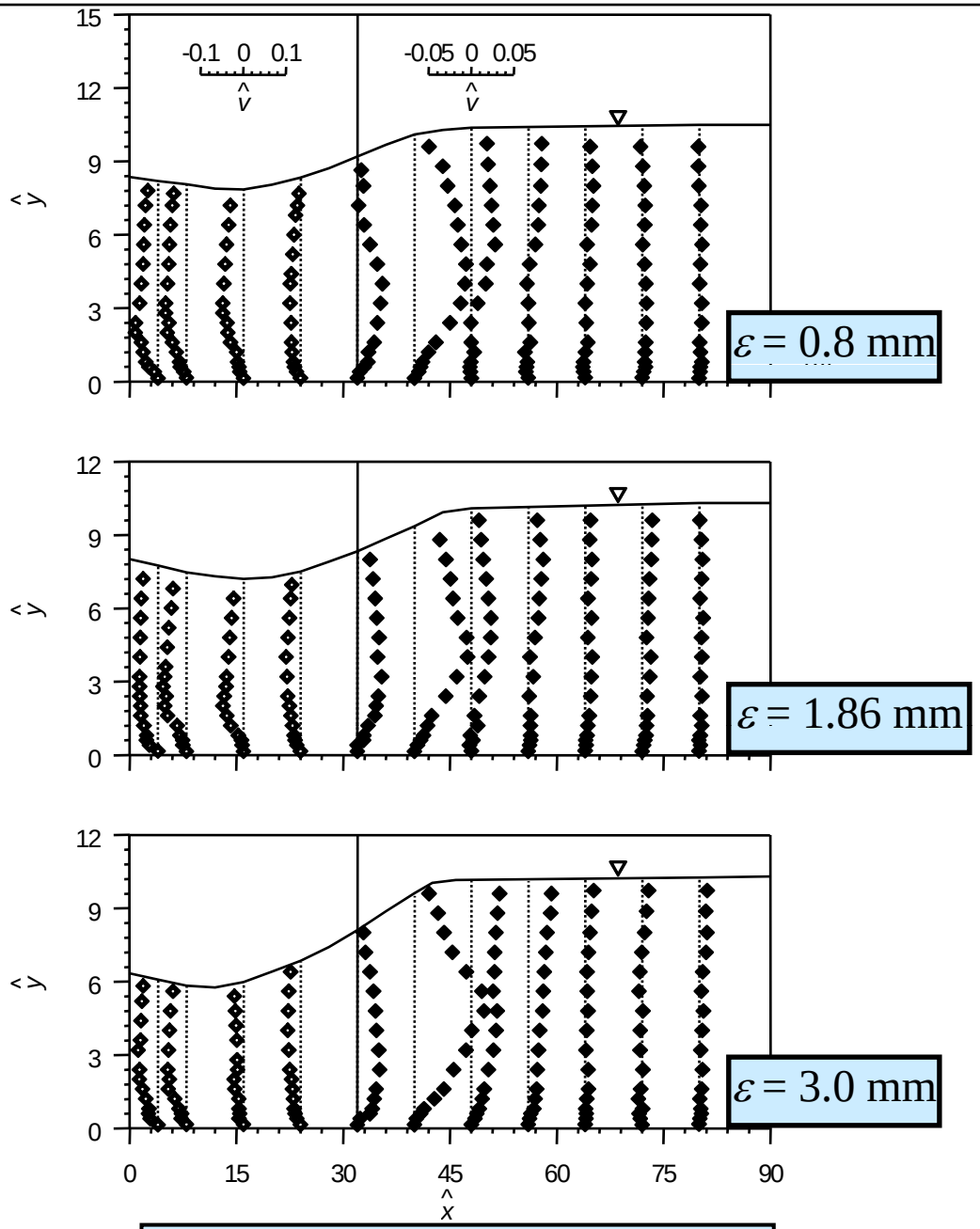

Vertical distributions of $\hat{v}$

- direction of v changes from downward to upward at the junction of the smooth and rough beds
- upward motion of the flow increases with increase in roughness ε on the rough beds
- frictional resistance exerted by the bed roughness on the submerged wall jet is distinguishable in the fully developed zone
- downward motion of the flow on the smooth bed indicates a strong surface roller

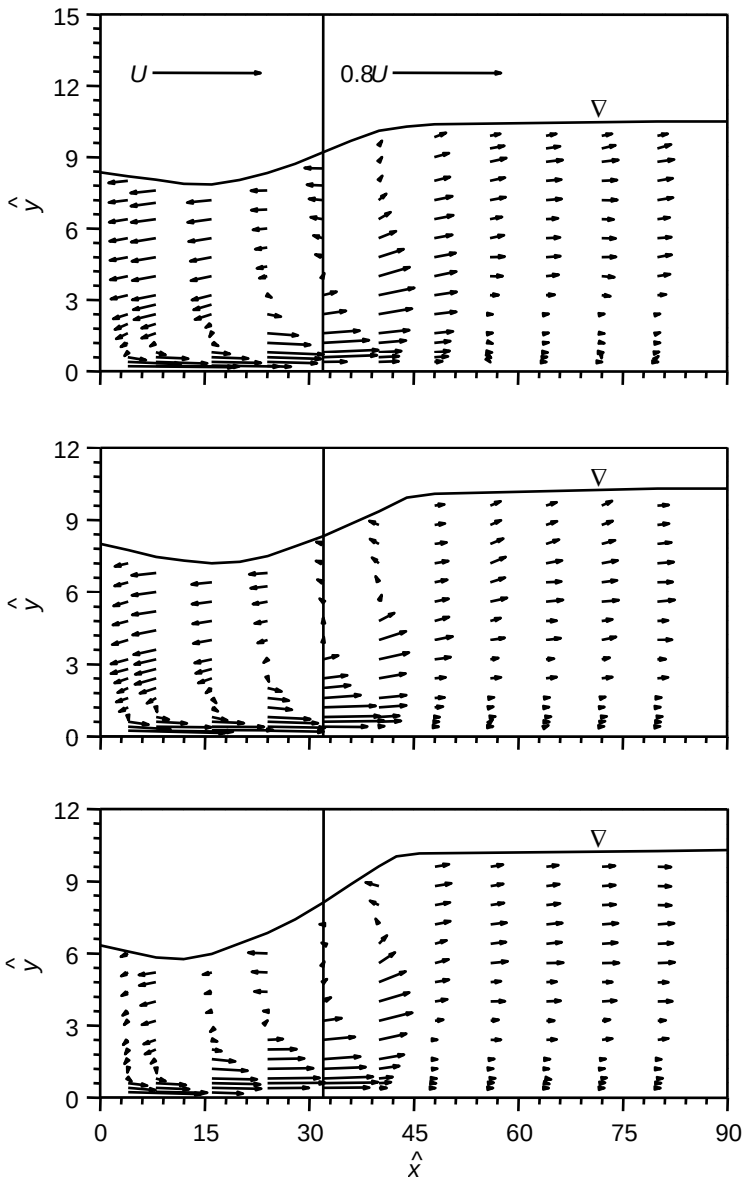

ε = 0.8 mm

ε = 1.86 mm

ε = 3.0 mm

Normalized velocity vectors

- characteristics of the jet diffusion including a swirl flow in the fully developed zone are evident
- no noticeable discontinuity in velocity distributions is observed
- behaviour is different from that observed in close-conduit flows, where an overshooting property was reported, possible reason being the variation of the free surface profile when an open channel flow is subjected to an abrupt change of bed roughness

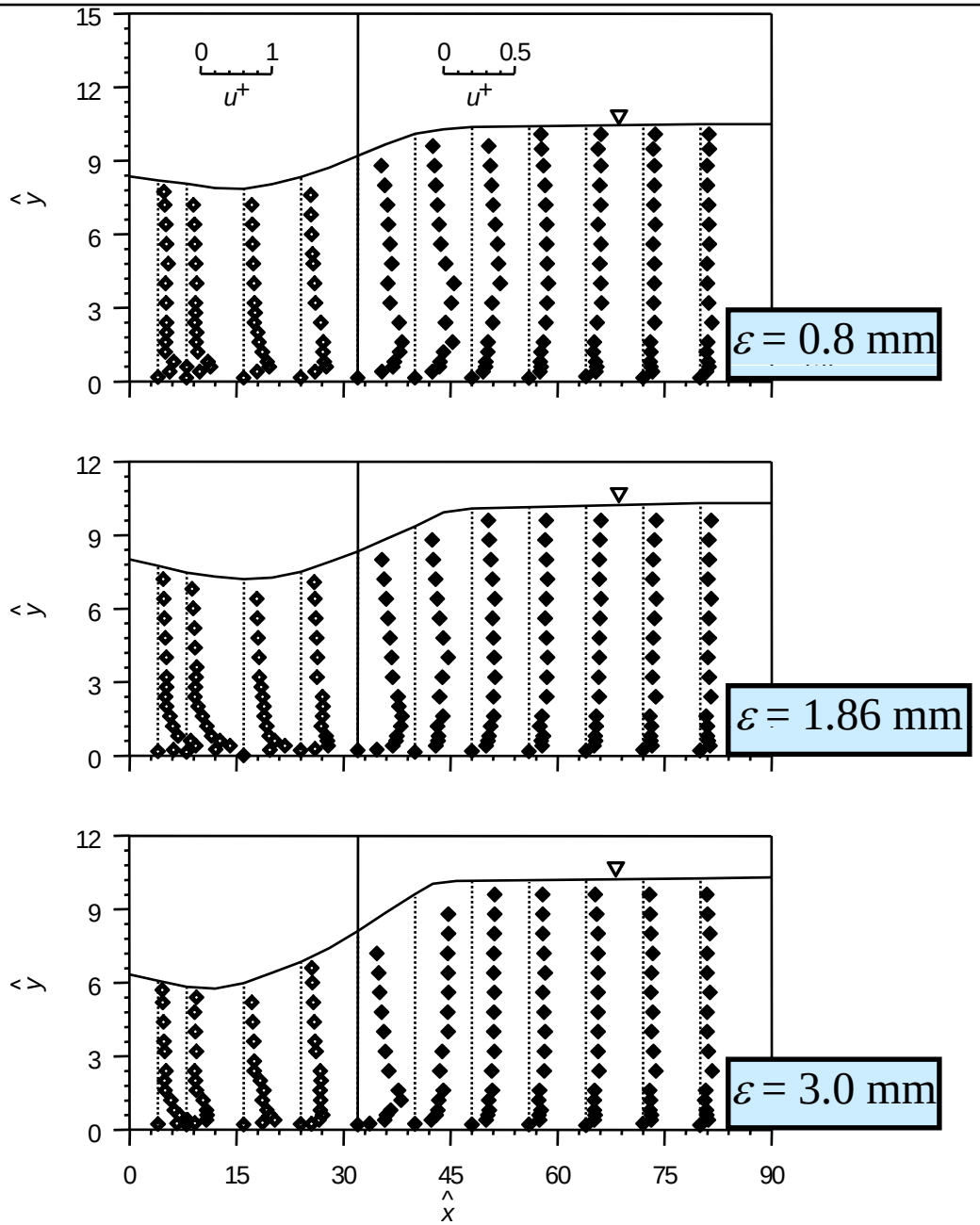

Vertical distributions of u^+

- pronounced bulges in the profiles of u^+ on the smooth bed are apparent as a result of reverse flow
- profiles of u^+ have continuity (that is the change is gradual) from smooth bed, in the fully developed zone
- in the recovering zone, u^+ increases with increase in $\hat{y}$ vertical distance over a short distance and then becoming constant over the entire zone
- local maximum value of u^+ of a vertical profile increases with increase in streamwise distance up to an overall maximum at the middle of the smooth bed

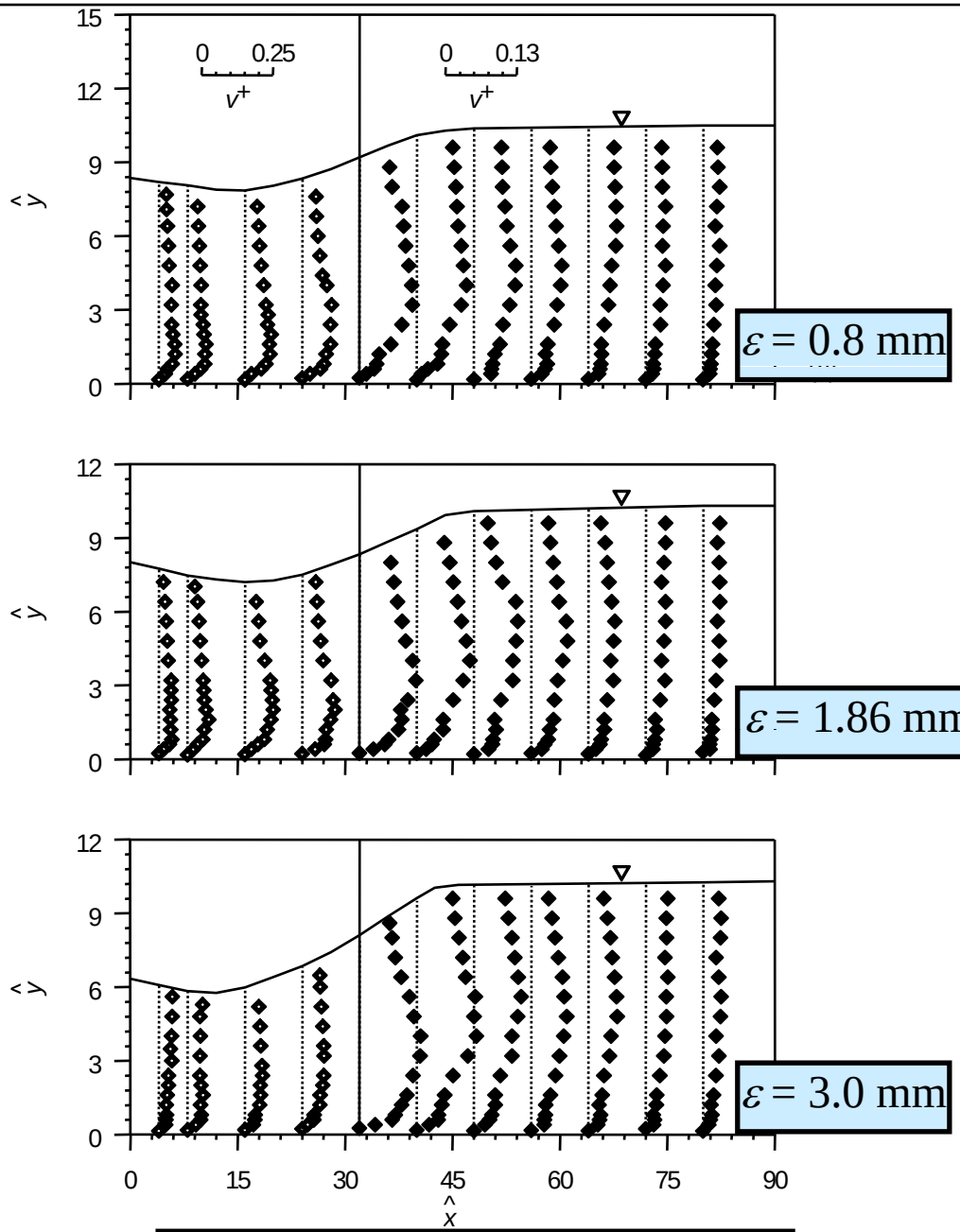

Vertical distributions of v^+

- bulges are also evident at the mid flow depth except near the sluice opening
- magnitude of v^+ of a particular profile increases with increase in bed roughness ε
- v^+ increases with increase in $\hat{x}$ up to the junction of the smooth and rough beds and then decreases to attain a constant profile in the recovering zone

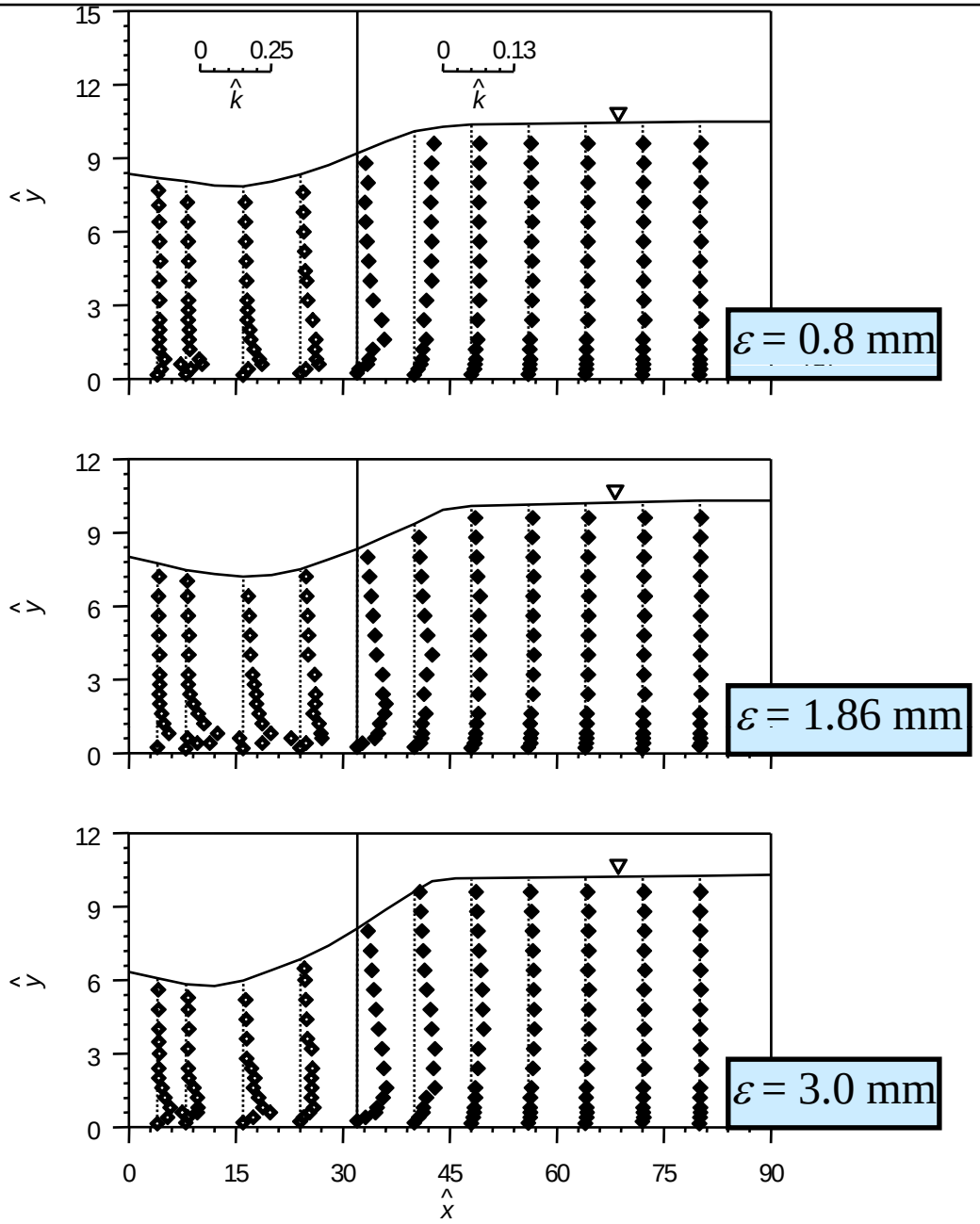

Vertical distributions of $\hat{k}$

- bulges are resulting from the reversal nature of the flow due to the surface roller in the fully developed zone, as the turbulent kinetic energy gets stronger
- change of the turbulence profiles is observed to be gradual at the junction of smooth and rough beds

Diffusion of submerged wall jet

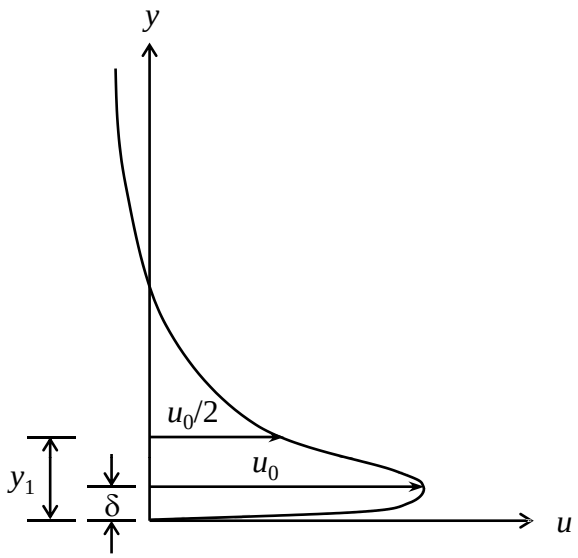

Typical velocity distribution

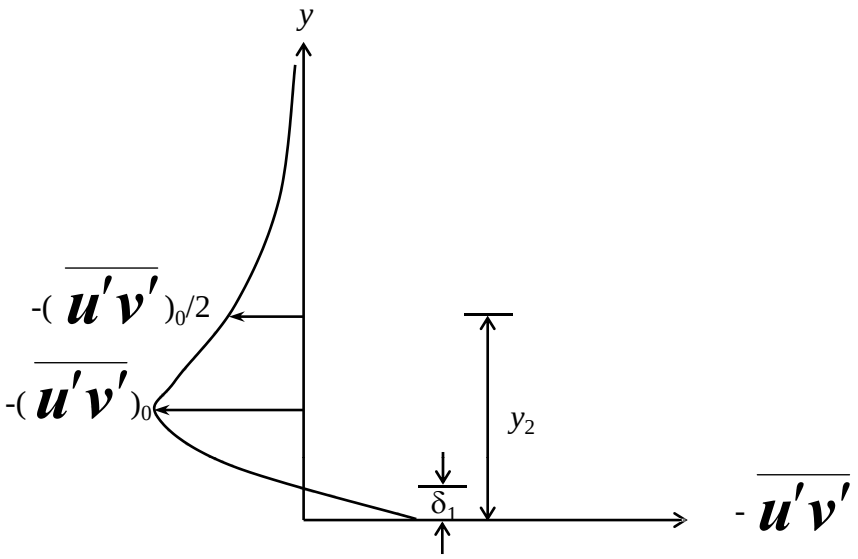

Reynolds stress distribution

• functional representation of the development of local maximum velocity u_0 and boundary layer thickness δ along streamwise distance x

$$u_0(x \le L) = u_0(U, b, x, \nu)$$
$$u_0(x > L) = u_0(U, b, x - L, \varepsilon)$$

(1)

$$\delta(x \le L) = \delta(U, b, x, \nu)$$
$$\delta(x > L) = \delta(U, b, x - L, \varepsilon)$$

(2)

• applying the dimensional analysis and physical reasoning and using multiple linear regressions of the experimental data collected by the ADV

$$\hat{u}_0(\hat{x} \le \hat{L}) = 1 - 0.235\hat{x}^{0.4} R^{-0.05}$$

$$\hat{u}_0(\hat{x} > \hat{L}) = 1 - 0.1(\hat{x} - \hat{L})^{0.55} \hat{\varepsilon}^{0.05}$$

(3)

$$\hat{\delta}(\hat{x} \le \hat{L}) = 0.27(\hat{x} + 11.2)^{0.72} R^{-0.2}$$

$$\hat{\delta}(\hat{x} > \hat{L}) = 0.21(\hat{x} - \hat{L})^{0.75} \hat{\varepsilon}^{0.25}$$

(4)

$\hat{u}_0 = u_0/U$; $\hat{\varepsilon} = \varepsilon/b$; $\hat{L} = L/b$ and $\hat{\delta} = \delta/b$

- virtual origin of the boundary layer of a jet lies at $x = -11.2b$ where $\delta = 0$ (Schwarz and Cosart 1961)
- Eqs. (3) and (4) indicate that the jet velocity diffuses and the boundary layer thickness increases with increase in streamwise distance x

Experimental Reynolds Stress

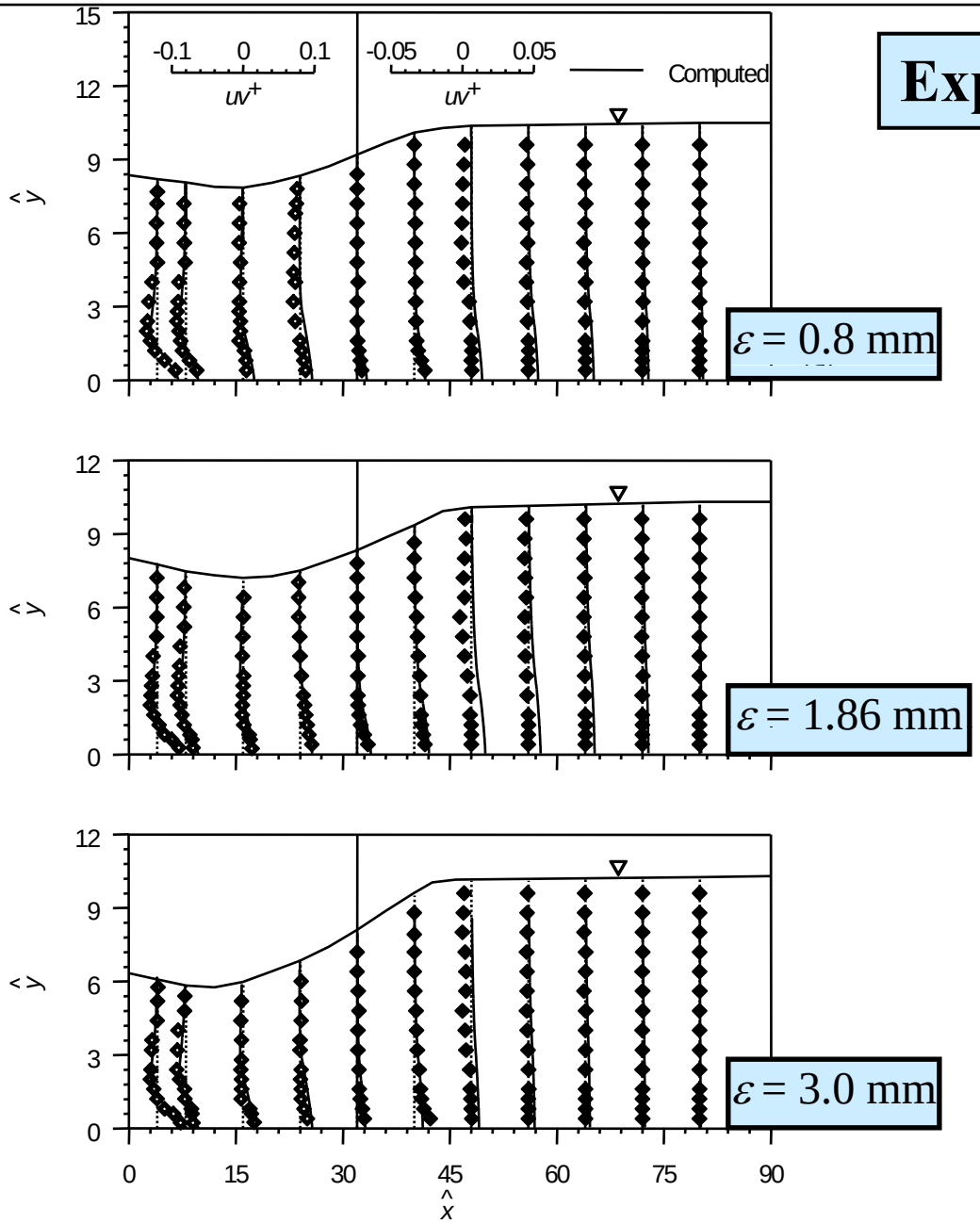

Vertical distributions of uv^+

- the Reynolds stress uv^+ near the bed is positive and reduces sharply changing its sign to negative and forming bulges with increase in vertical distance due to the surface roller on the smooth bed
- bulges in the profiles of uv^+ gradually disappear with increase in $\hat{x}$
- in the recovering zone, uv^+ being feeble is almost constant along the vertical

Theoretical Determination of Reynolds Stress

• two-dimensional Navier-Stokes equations of a steady turbulent flow are given in nondimensional form

$$\hat{u}\frac{\partial \hat{u}}{\partial \hat{x}} + \hat{v}\frac{\partial \hat{u}}{\partial \hat{y}} = -\frac{\partial \hat{p}}{\partial \hat{x}} + \frac{1}{R}\left(\frac{\partial^2 \hat{u}}{\partial \hat{x}^2} + \frac{\partial^2 \hat{u}}{\partial \hat{y}^2}\right) - \frac{\partial u^{+2}}{\partial \hat{x}} - \frac{\partial uv^{+}}{\partial \hat{y}} \qquad (5)$$

$$\hat{u}\frac{\partial \hat{v}}{\partial \hat{x}} + \hat{v}\frac{\partial \hat{v}}{\partial \hat{y}} = -\frac{\partial \hat{p}}{\partial \hat{y}} + \frac{1}{R}\left(\frac{\partial^2 \hat{u}}{\partial \hat{x}^2} + \frac{\partial^2 \hat{u}}{\partial \hat{y}^2}\right) - \frac{\partial v^{+2}}{\partial \hat{y}} - \frac{\partial uv^{+}}{\partial \hat{x}} \qquad (6)$$

• $\hat{p} = p/(\rho U^2)$; p = piezometric pressure; ρ = mass density of fluid; $R = Ub/\nu$, that is the Reynolds number of issuing jet; and ν = kinematic viscosity of fluid

- **continuity equation**

$$\frac{\partial \hat{u}}{\partial \hat{x}} + \frac{\partial \hat{v}}{\partial \hat{y}} = 0 \qquad (7)$$

- applying the boundary layer approximation for submerged jets

$$\hat{u}\frac{\partial \hat{u}}{\partial \hat{x}} + \hat{v}\frac{\partial \hat{u}}{\partial \hat{y}} + \frac{\partial}{\partial \hat{x}}(u^{+2} - v^{+2}) + \frac{\partial uv^{+}}{\partial \hat{y}} = \frac{1}{R}\frac{\partial^2 \hat{u}}{\partial \hat{y}^2} \qquad (8)$$

- as flow in submerged jets is self-preserving by nature, the following functions can be considered

$$\hat{u} = \hat{u}_0\,\psi(\eta) \qquad (9)$$

$$u^{+2} = \hat{u}_0^2\,\phi_1(\eta) \qquad (10)$$

$$\eta = \hat{y}/\hat{\delta}$$

$$v^{+2} = \hat{u}_0^2\,\phi_2(\eta) \qquad (11)$$

$$uv^{+} = -\hat{u}_0^2\,\xi(\eta) \qquad (12)$$

$$\frac{\hat{\delta}}{\hat{u}_0}\frac{\partial \hat{u}_0}{\partial \hat{x}}\psi^2 - \frac{1}{\hat{u}_0}\frac{d(\hat{u}_0\hat{\delta})}{d\hat{x}}\frac{d\psi}{d\eta}\int_0^{\eta}\psi d\eta + 2\frac{\hat{\delta}}{\hat{u}_0}\frac{d\hat{u}_0}{d\hat{x}}\phi_1 - \frac{d\hat{\delta}}{d\hat{x}}\eta\frac{d\phi_1}{d\eta} + \frac{d\hat{\delta}}{d\hat{x}}\eta\frac{d\phi_2}{d\eta}$$

$$-2\phi_2\frac{\hat{\delta}}{\hat{u}_0}\frac{d\hat{u}_0}{d\hat{x}} - \frac{d\xi}{d\eta} = \frac{1}{R}\frac{d^2\psi}{d\eta^2} \qquad (13)$$

- Integrating Eq. (13) and neglecting the viscous term, the equation of nondimensional Reynolds stress uv^+

$$uv^+ = -\hat{u}_0\hat{\delta}\frac{d\hat{u}_0}{d\hat{x}}\int_{\eta}^{\hat{h}}\psi^2 d\eta - \hat{u}_0\left(\hat{\delta}\frac{d\hat{u}_0}{d\hat{x}} + \hat{u}_0\frac{d\hat{\delta}}{d\hat{x}}\right)\left(\int_{\eta}^{\hat{h}}\psi^2 d\eta + \psi\int_0^{\eta}\psi d\eta\right) \qquad (14)$$

$\hat{h} = h/b$; and h = flow depth at any x

$\psi = \psi(\eta)$ can be obtained from the similarity of u distributions at different streamwise distances x

$$\psi(\eta \le 1) = \eta^{1/\alpha}$$ (15)

$$\psi(\eta > 1) = \exp[c(\eta - 1)^{0.95}]$$ (16)

ε (mm)	c	α	β	σ
Smooth bed	-1.41	7.81	1.308	0.641
0.8	-1.12	5.42	1.048	0.426
1.86	-0.93	5.05	0.862	0.412
3	-0.9	4.95	0.642	0.397

computed profiles of uv^+, in general, agree satisfactorily with the experimental data

Theoretical Determination of Bed Shear Stress

- Using Eqs. (7), (9), (10), (11), (12) in (8) and integrating

$$\hat{\tau} = -\left(2\hat{\delta}\hat{u}_0 \frac{d\hat{u}_0}{d\hat{x}} + \hat{u}_0^2 \frac{d\hat{\delta}}{d\hat{x}} \right) \int_0^{\eta} (\psi^2 + \phi_1 - \phi_2) d\eta \qquad (17)$$

- Using the present experimental data, the expressions $\phi_1 = \eta^{1/\beta}$ and $\phi_2 = \eta^{1/\sigma}$ are fitted for different rough beds

Experimental Determination of Bed Shear Stress

- Bed shear stress τ can be determined experimentally from the Reynolds stress distribution extending it on to the bed level

- The nondimensional bed shear stress is given by

$$\hat{\tau} = \boldsymbol{uv}^{+}\Big|_{\hat{y}=0} \qquad (18)$$

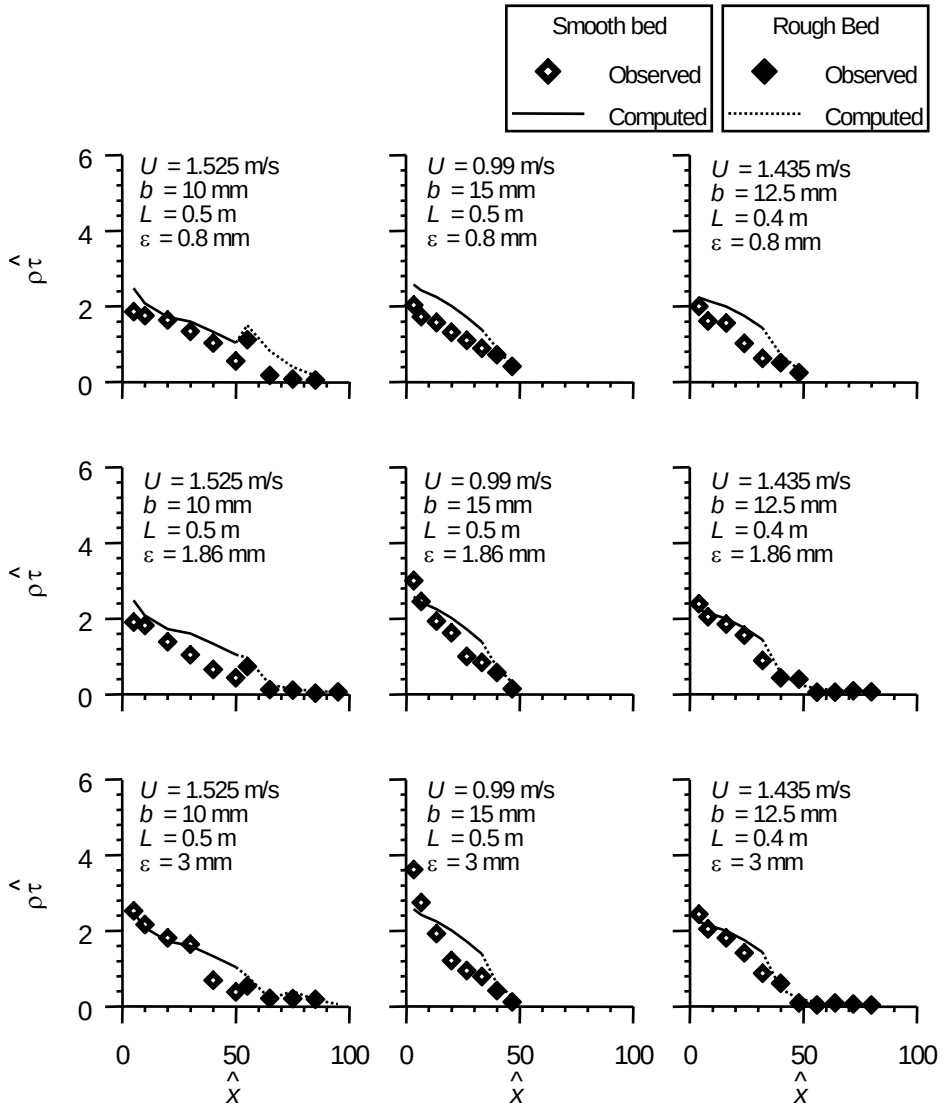

Horizontal distributions of $\rho\hat{\tau}$

- though there is a tendency of overestimating the measured bed shear stress in the smooth beds, in general, computed bed shear stresses correspond closely with the experimentally obtained bed shear stresses
- bed shear stress τ decreases with increase in streamwise distance x
- change of τ at the junction of smooth and rough beds are gradual, though on a few occasions a slight discontinuity is observed

Determination of Length Scale

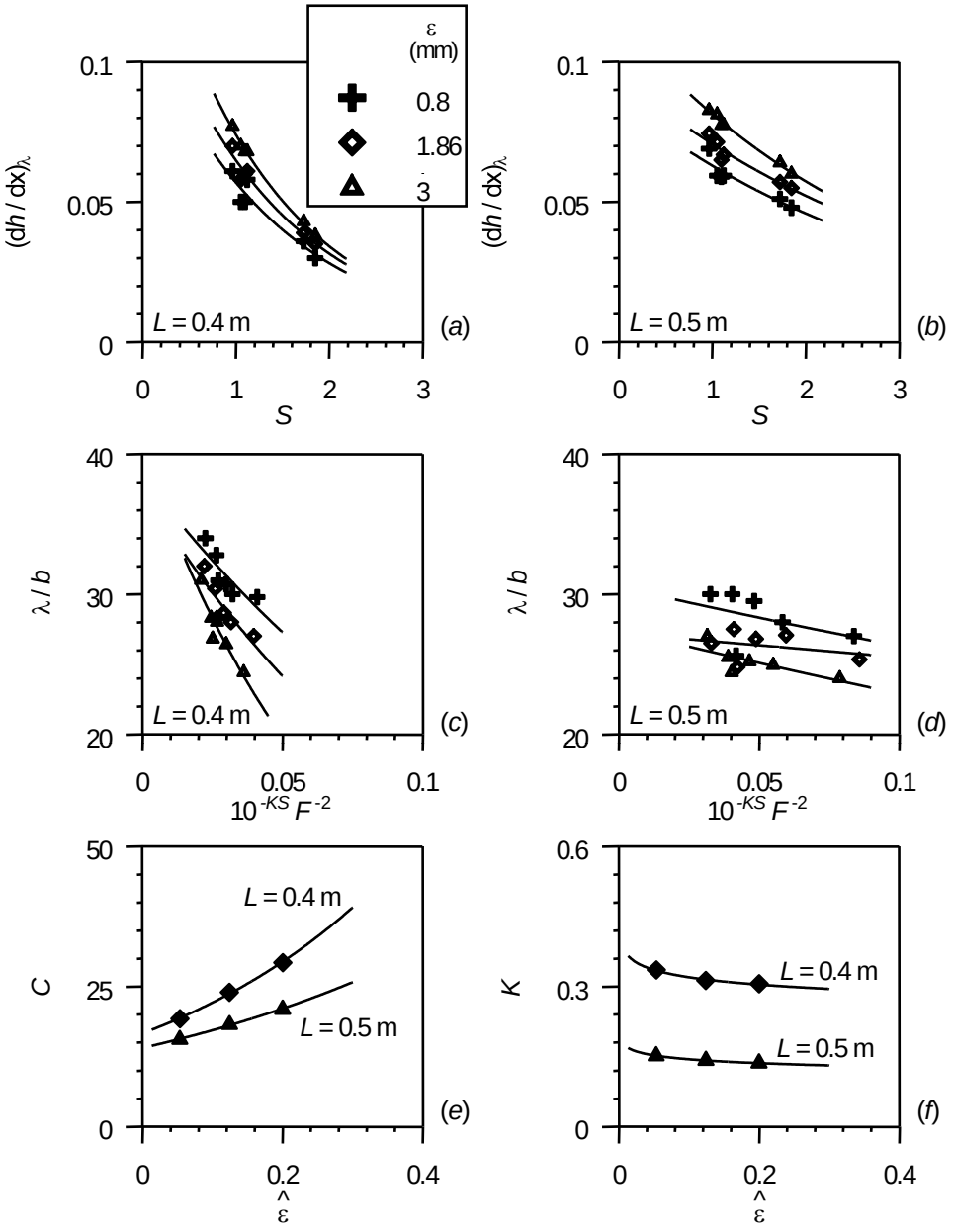

- Long et al. (1990) introduced a length scale λ for local maximum jet velocity u_0

$$\frac{\lambda}{b} = \frac{49}{1 + C_1 (dh/dx)_\lambda F^{-2}} \qquad (19)$$

- argued that the free surface slope at $x = \lambda$, that is $(dh/dx)_\lambda$, is influenced by the submergence factor S

- but with rough beds, $(dh/dx)_\lambda$ is a function of S, L and ε

$$\left(\frac{dh}{dx}\right)_\lambda = C_2 10^{-KS} \qquad (20)$$

$$\frac{\lambda}{b} = \frac{49}{1 + C 10^{-KS} F^{-2}} \qquad (21)$$

- barring horizontal length scale λ, the vertical length scale y_1 for velocity u, which is the vertical distance y where $u = u_0/2$ and $\partial u/\partial y < 0$, is used to bring down the vertical distributions of $\hat{\boldsymbol{u}}$ on a single band
- vertical length scale y_2 for the Reynolds stress $-\overline{\boldsymbol{u}'\boldsymbol{v}'}$, being the vertical distance y where $\overline{\boldsymbol{u}'\boldsymbol{v}'} = (\overline{\boldsymbol{u}'\boldsymbol{v}'})_0/2$ and $\partial(\overline{\boldsymbol{u}'\boldsymbol{v}'})/\partial y < 0$, is considered to group the vertical distributions of uv^+ together
- for the null-point of the Reynolds stress profiles, $y = \delta_1$ where $\overline{\boldsymbol{u}'\boldsymbol{v}'} = 0$ and $\partial(\overline{\boldsymbol{u}'\boldsymbol{v}'})/\partial y > 0$

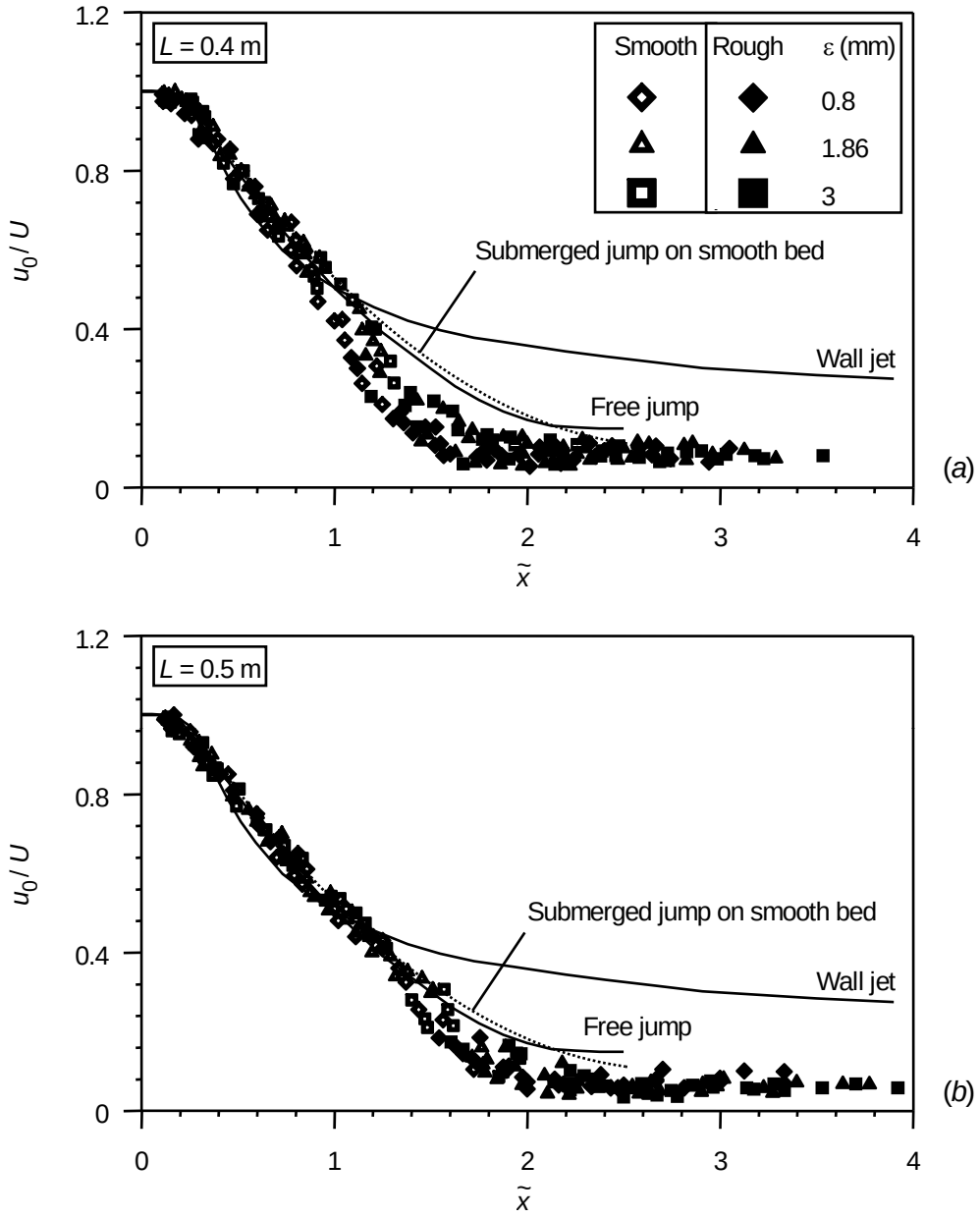

$\tilde{x} = x/\lambda$

Flow Characteristics

- use of a common length

- decay rate of local maximum velocity u_0, being notably influenced by the bed roughness, increases on rough beds
- flow is self-preserving on smooth and rough beds
- increase of the length of smooth bed L delays the decay rate

smooth bed

- data on rough bed region lie well below the curves of free jump and submerged jump on smooth bed

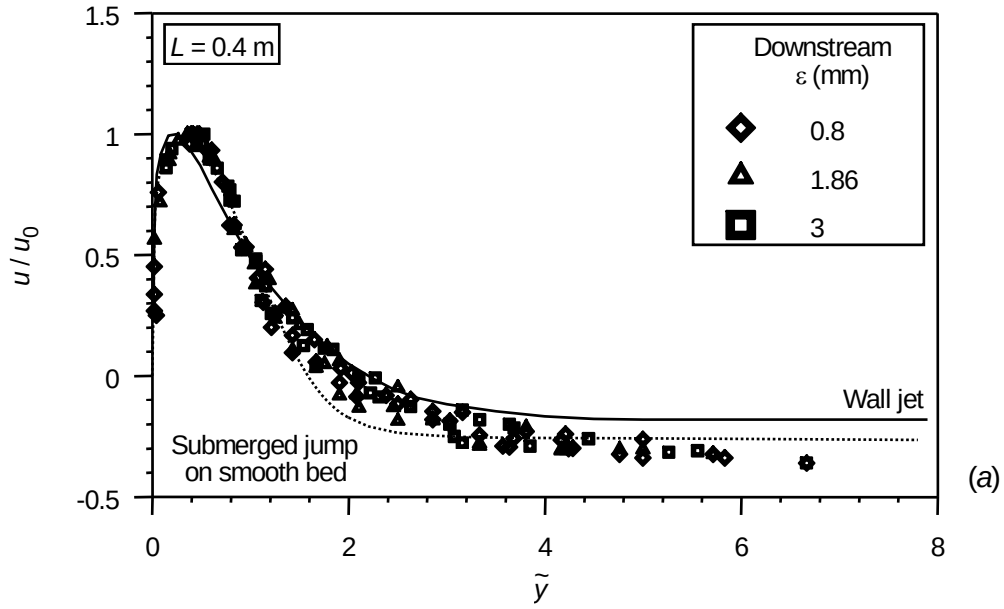

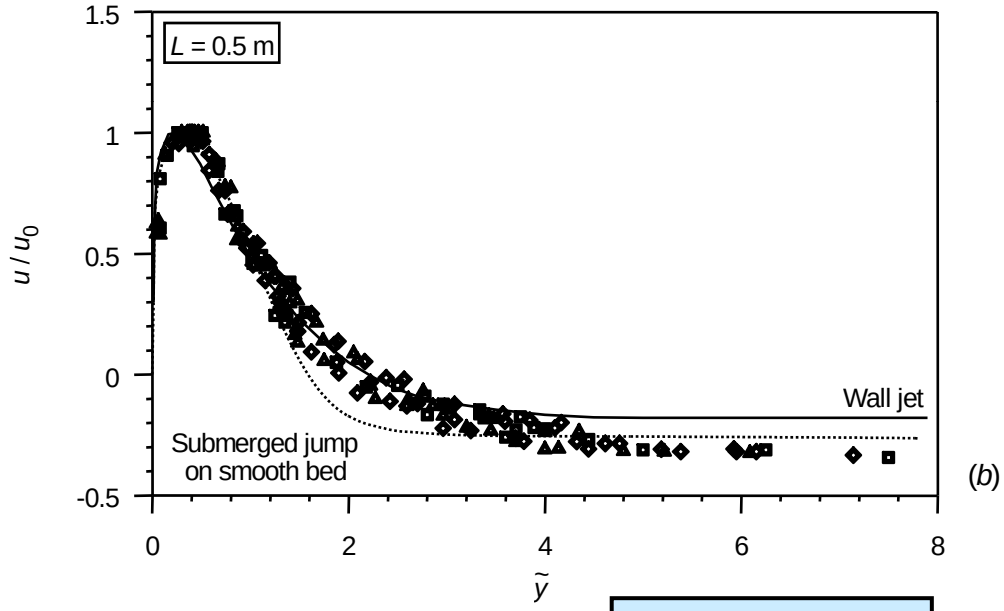

$\tilde{y} = y/y_1$

- collapse of the velocity data and the curves of wall jet and submerged jump on smooth bed is good up to $\tilde{y} =$ 1.5 for different L and downstream roughness ε
- velocity data have a departure from the wall jet curve in the outer-layer of velocity profiles for $\tilde{y} > 1.5$
- negative magnitude of u/u_0 in the profiles of the outer-layer indicates the region of reverse flow

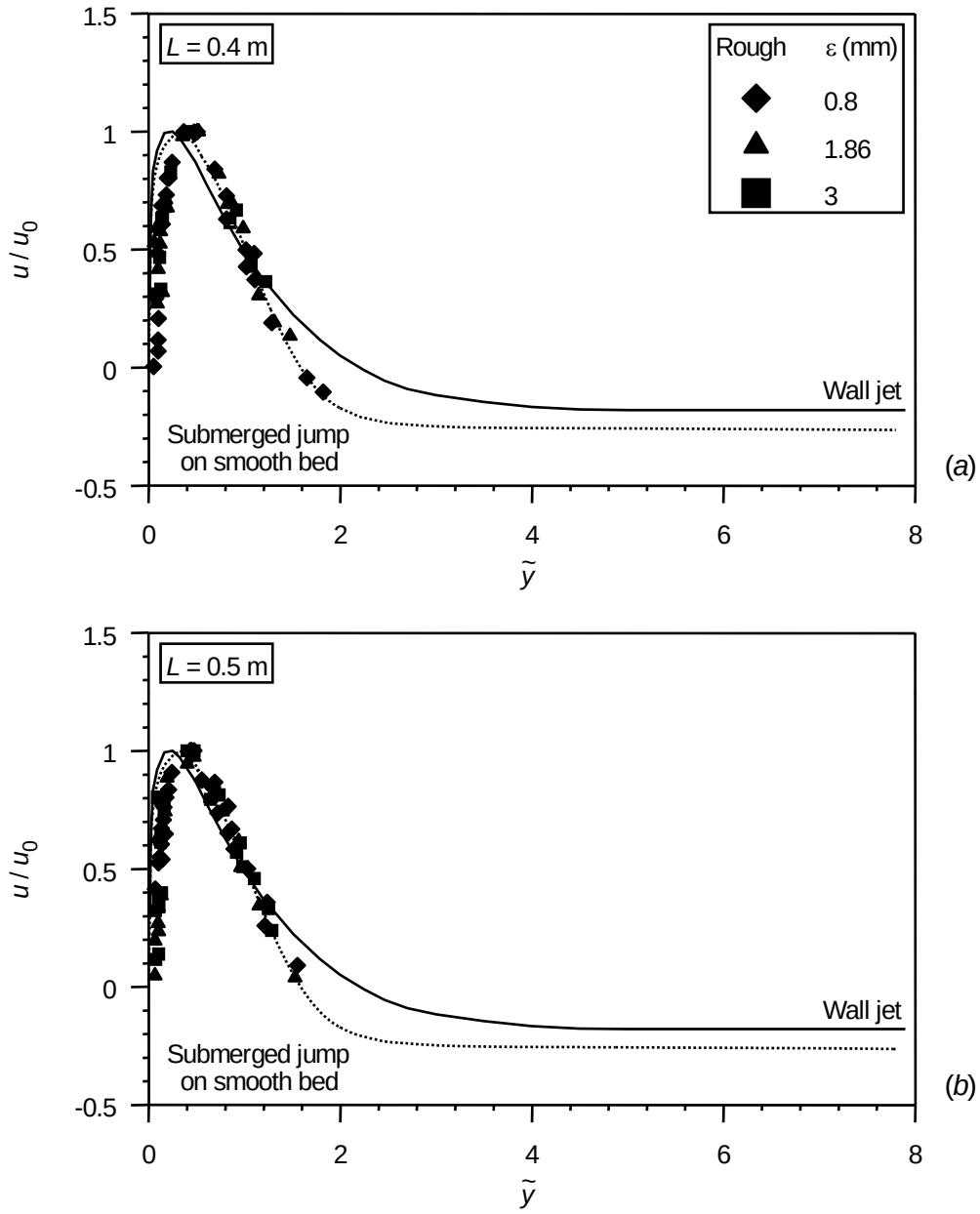

- bed roughness increases the inner-layer thickness of individual velocity profiles
- rough bed data near the bed are less “full” compared with the curves of wall jet and submerged jump on smooth bed

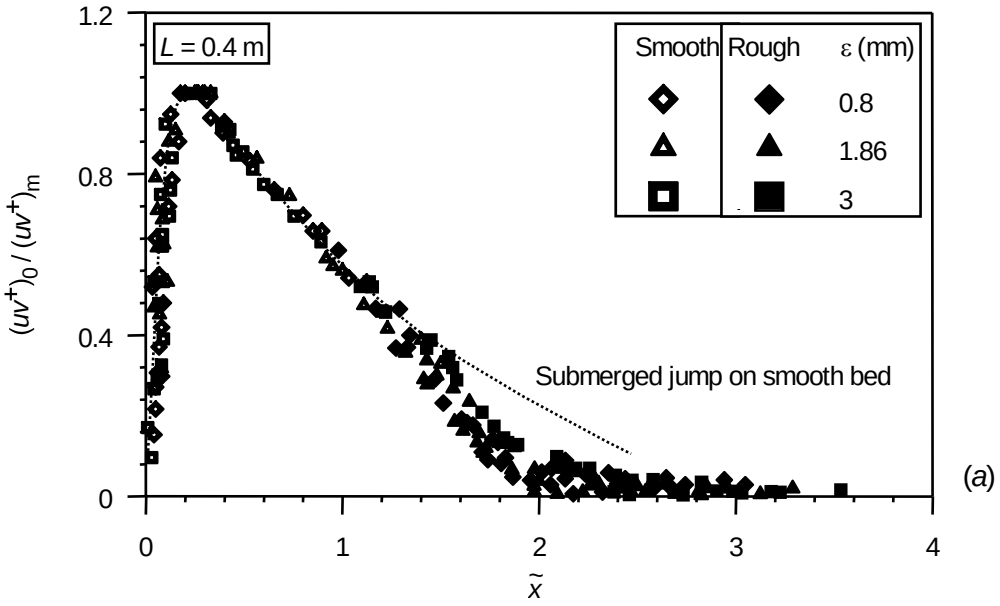

(*a*)

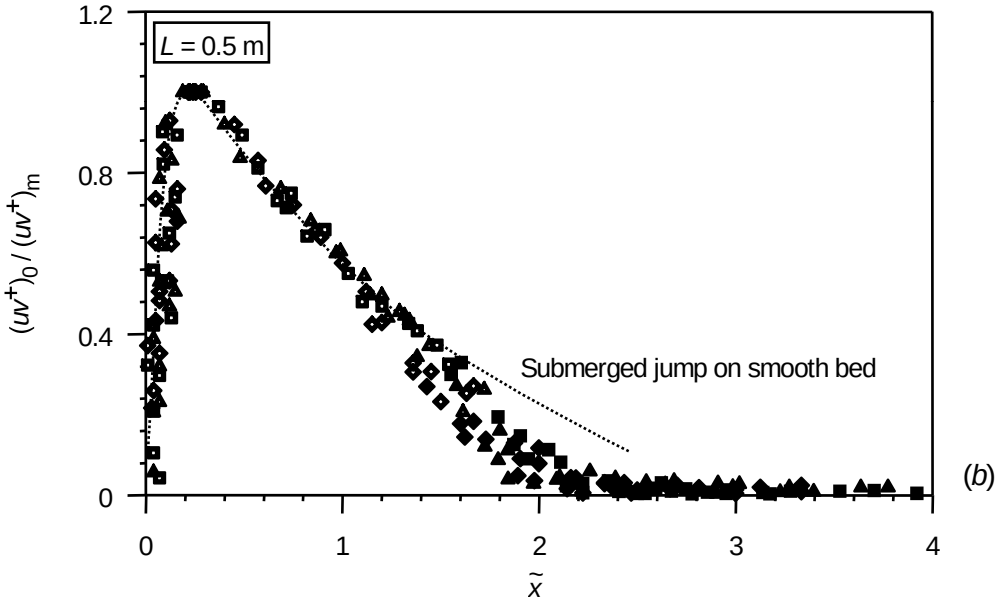

(*b*)

- little scatter in the vicinity of the junction of smooth and rough beds
- data trends have a considerable agreement with the curve of submerged jump on smooth bed in the smooth bed region
- data lie below the curve of submerged jump on smooth bed in the rough bed region due to the effect of roughness
- decay of $(uv^+)_0$ on rough beds are faster than those on smooth bed, as a result of mixing of fluid due to the roughness

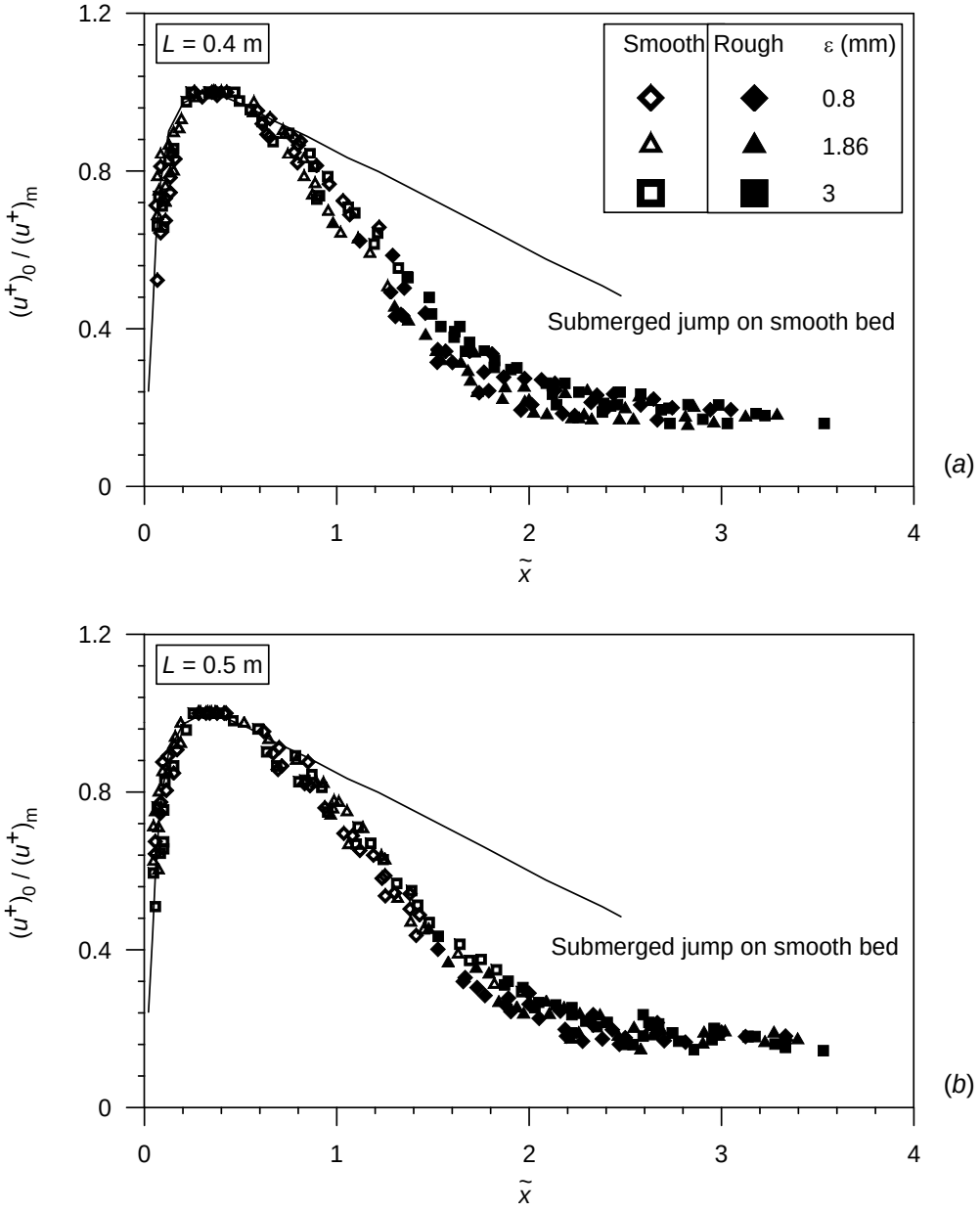

- scatter in the transition of the smooth and rough beds
- data trends have a considerable agreement with the curve of submerged jump on smooth bed in the smooth bed region
- data lie below the curve of submerged jump on smooth bed in the rough bed region due to the effect of roughness
- decay of $(u^+)_0$ on rough beds are faster than those on smooth bed, as a result of mixing of fluid due to the roughness

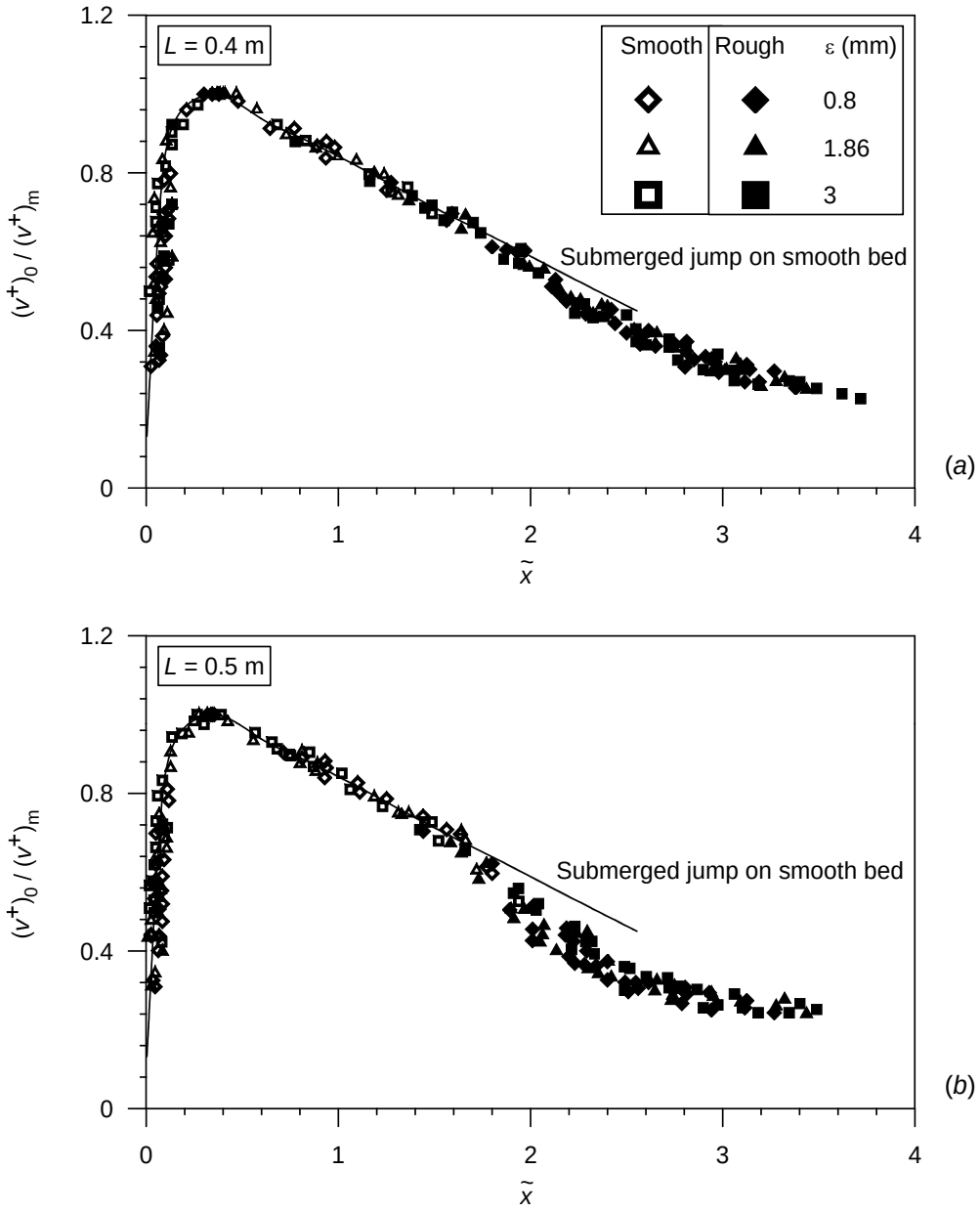

- little scatter in the vicinity of the junction of smooth and rough beds
- data trends have a considerable agreement with the curve of submerged jump on smooth bed in the smooth bed region
- data lie below the curve of submerged jump on smooth bed in the rough bed region due to the effect of roughness
- decay of $(v^+)_0$ on rough beds are faster than those on smooth bed, as a result of mixing of fluid due to the roughness

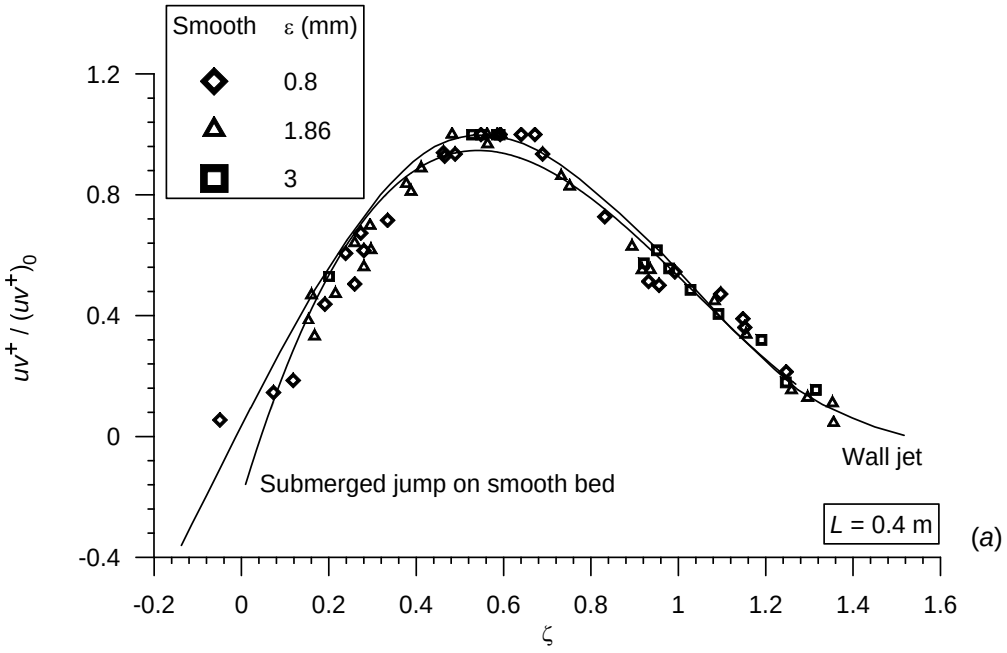

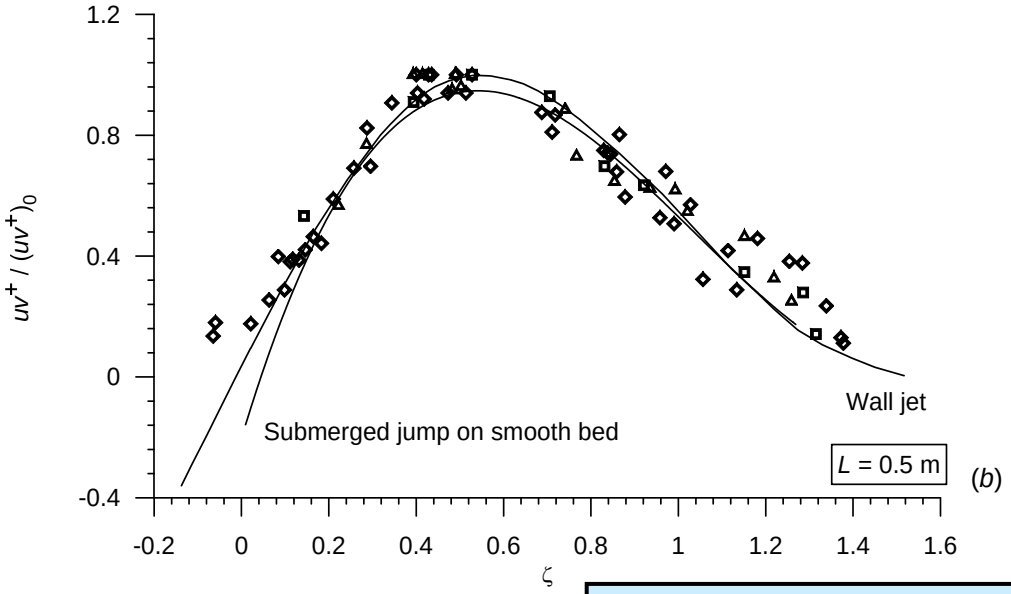

- data of smooth bed regions and the curves of submerged jump on smooth bed collapse in the inner-layer

$$\zeta = (y - \delta_1)/(y_2 - \delta_1)$$

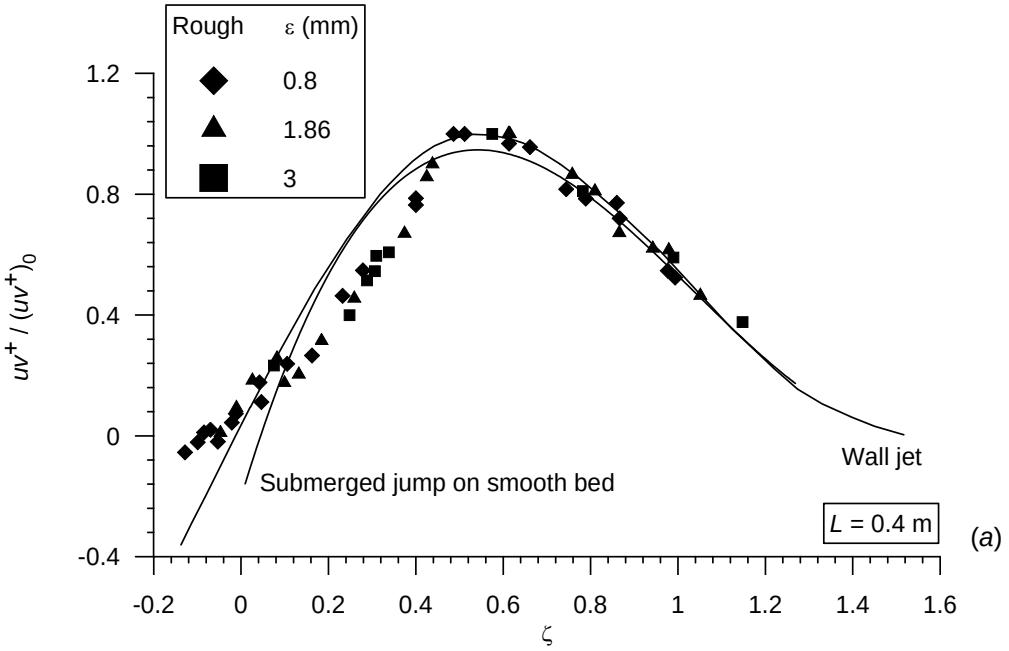

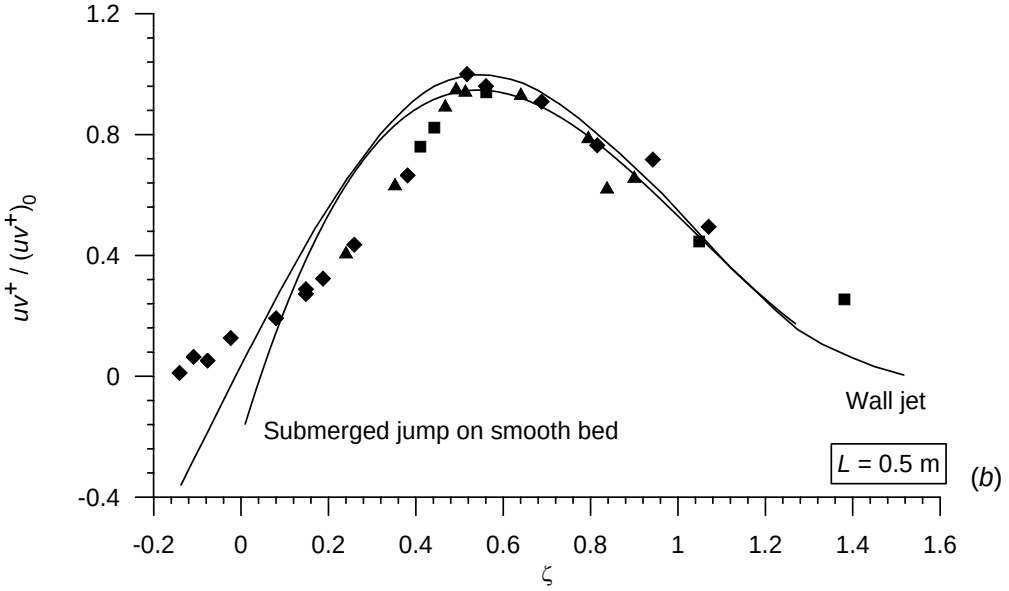

$$\zeta = (y - \delta_1)/(y_2 - \delta_1)$$

- data of $(uv^+)_0$ of rough bed regions, being sagging in nature, cross wall jet curve at $\zeta = 0.05$

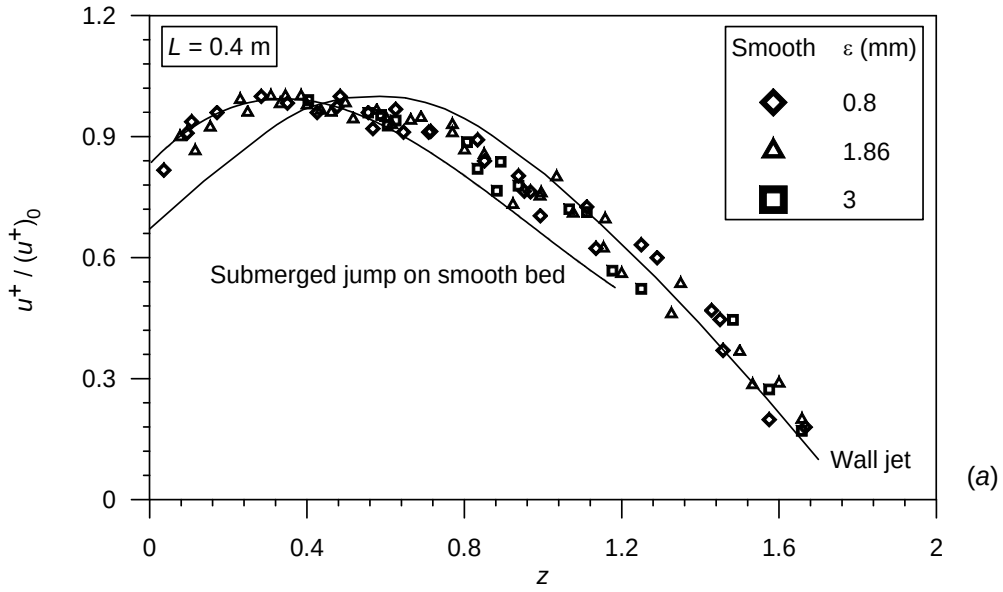

(*a*)

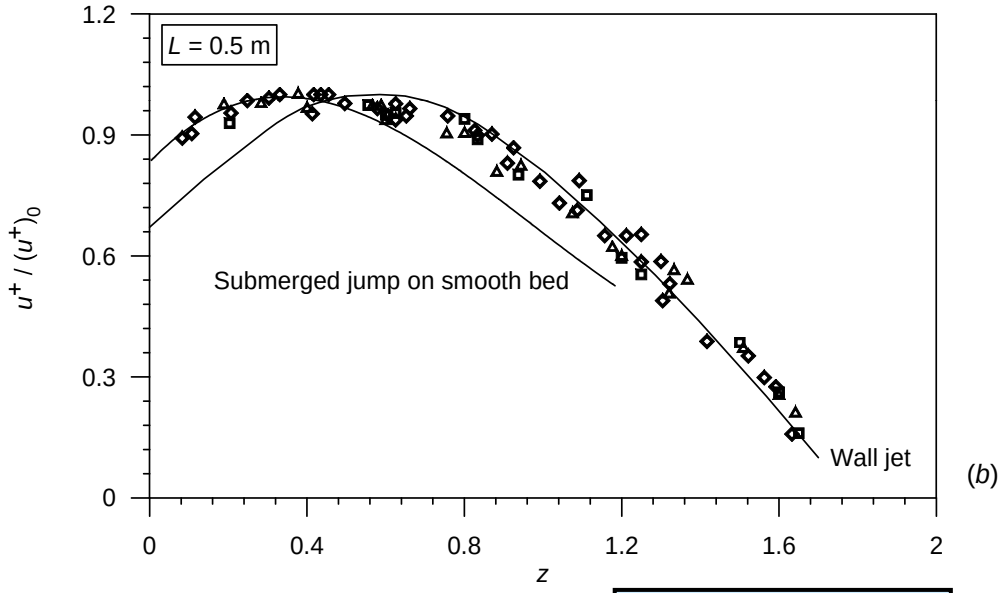

(*b*)

- data of $(u^+)_0$ of rough bed regions lie in between the curves of wall jet and submerged jump on smooth bed in the inner-layer

$z = y/y_2$

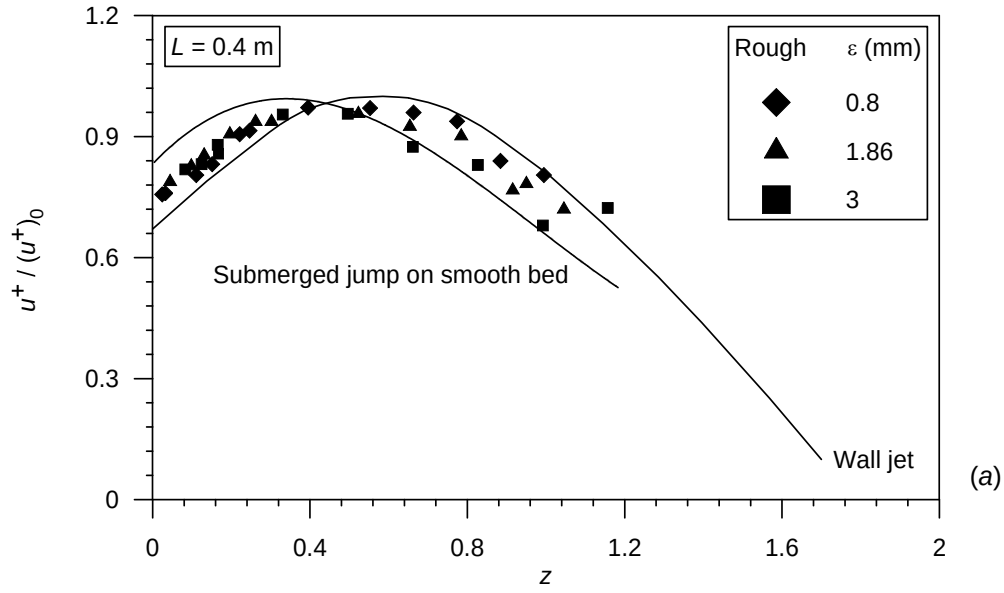

(*a*)

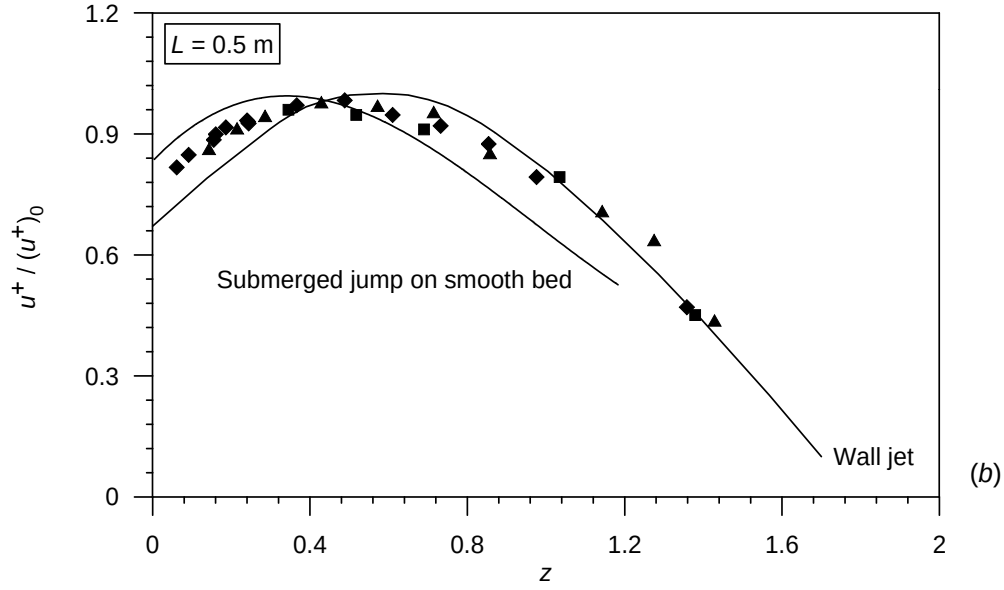

(*b*)

- roughness increases the inner-layer thickness of u^+

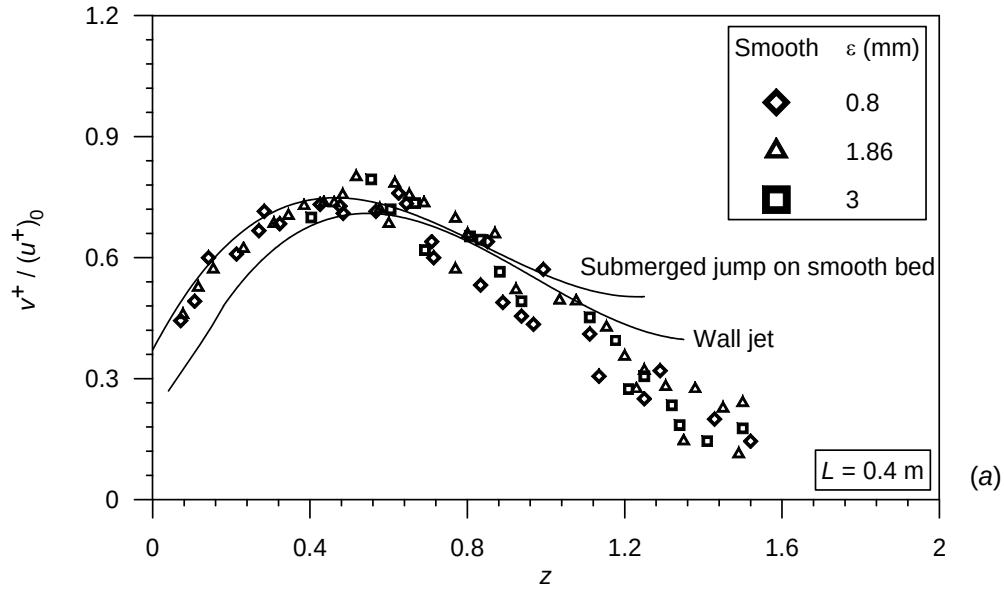

(*a*)

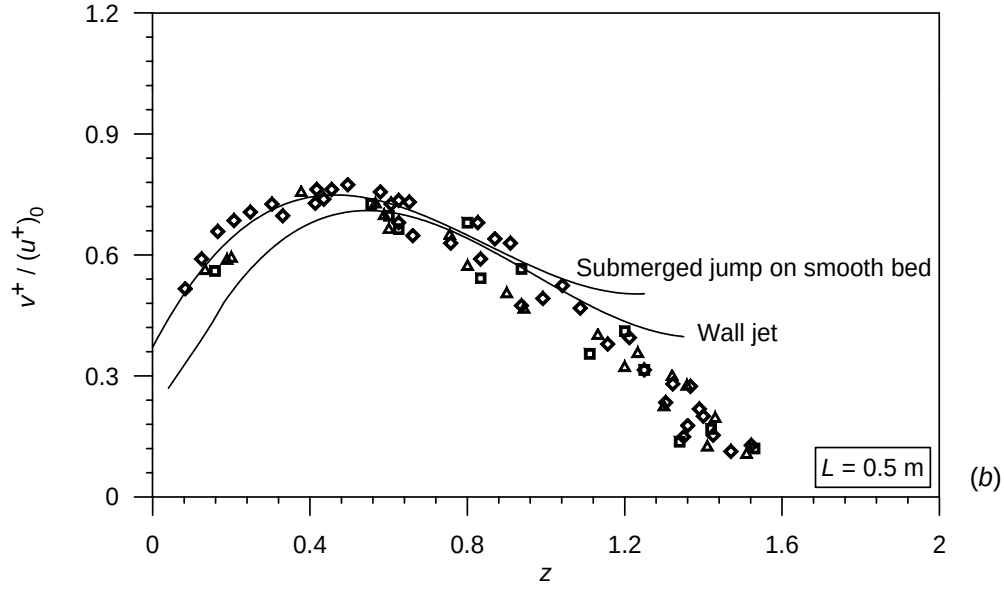

(*b*)

- data of $(v^+)_0$ of rough bed regions lie in between the curves of wall jet and submerged jump on smooth bed in the inner-layer

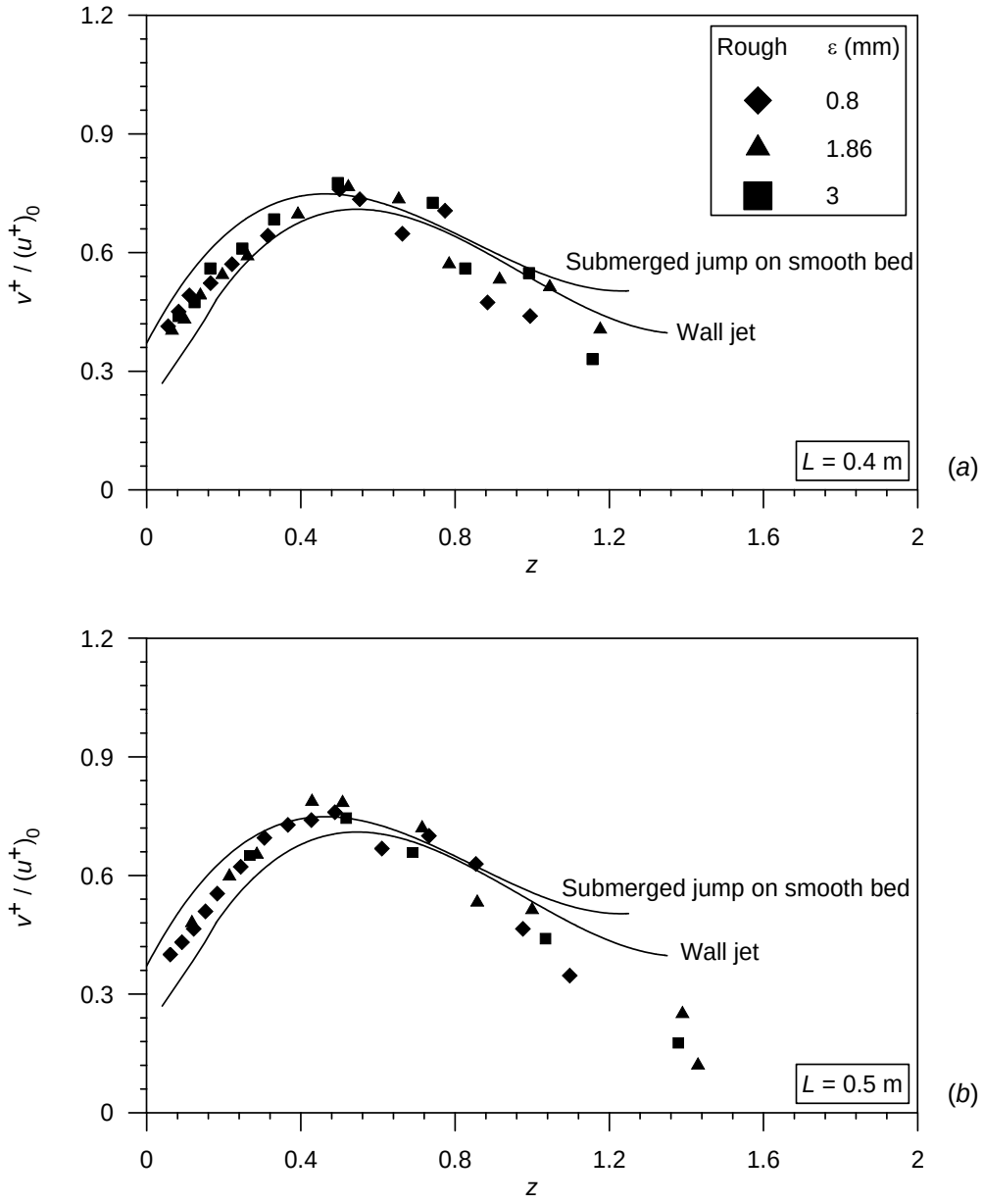

- roughness increases the inner-layer thickness of v^+

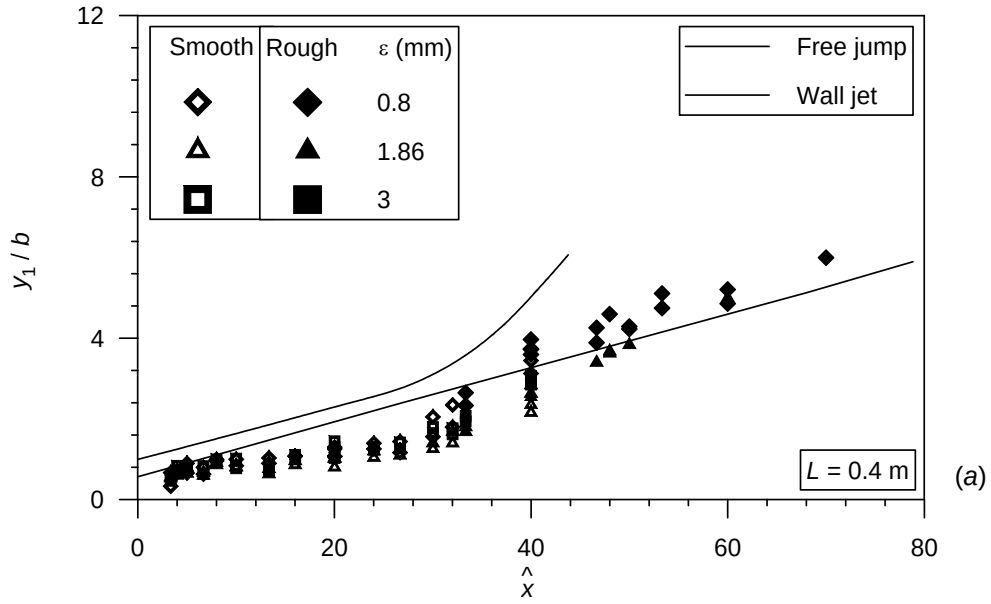

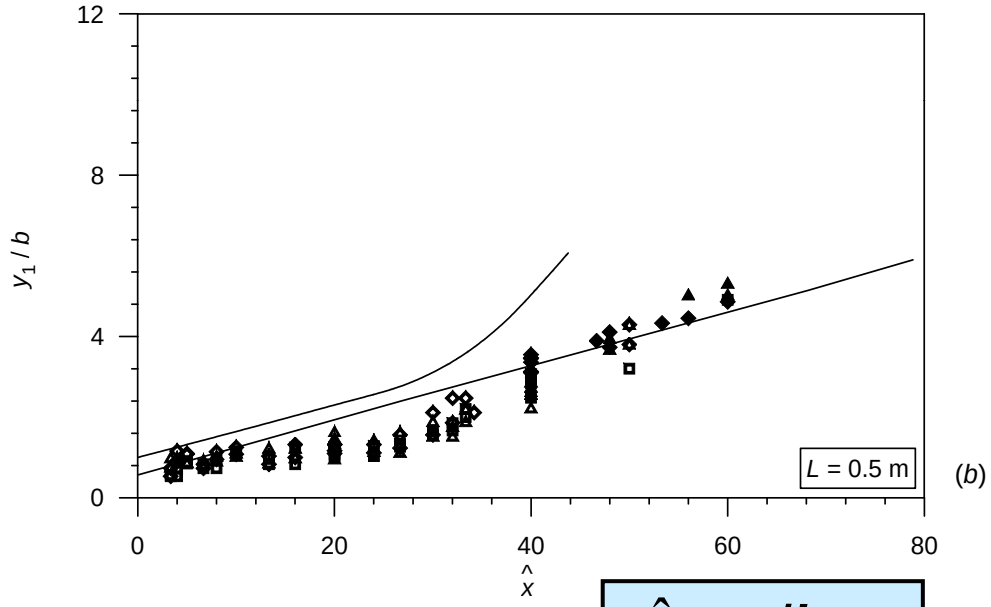

$\hat{x} = x/b$

- jet half-widths on smooth and rough beds diffuse slower and faster than that in classical wall jet, respectively
- jet half-width is influenced significantly by an abrupt change of bed roughness
- data lie well below the curve of free jump

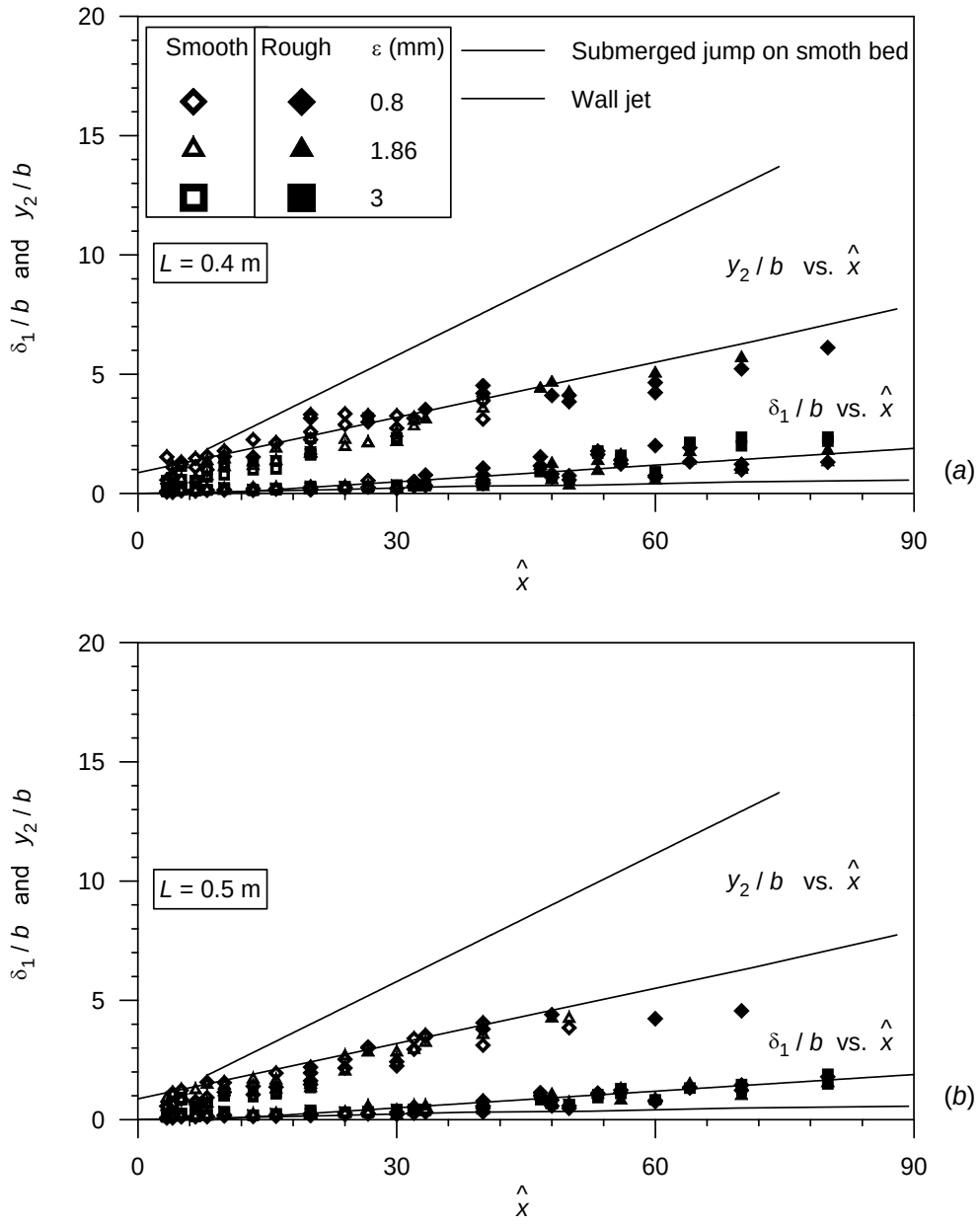

- half-width of the Reynolds stress on smooth and rough beds diffuses slower than those in the wall jet and submerged jump on smooth bed
- null-points of the Reynolds stress profiles in smooth and rough beds remain similar to that in submerged jet on smooth bed

Modelling of Scour Downstream of an Apron

Experimental Observation on Scour Process

- scour initiates at the downstream edge of the apron
- temporal variation of the vertical dimension of scour hole was faster than the longitudinal one
- in the initial stage, the suspension of sediments, in addition to the bed load, was the main means of sediment transport
- with the development of the vertical dimension of scour hole, the mode of sediment transport changed to the bed load only
- upstream portion of the scour hole achieved a steeper slope than the downstream portion

Equilibrium of Sediment Particles

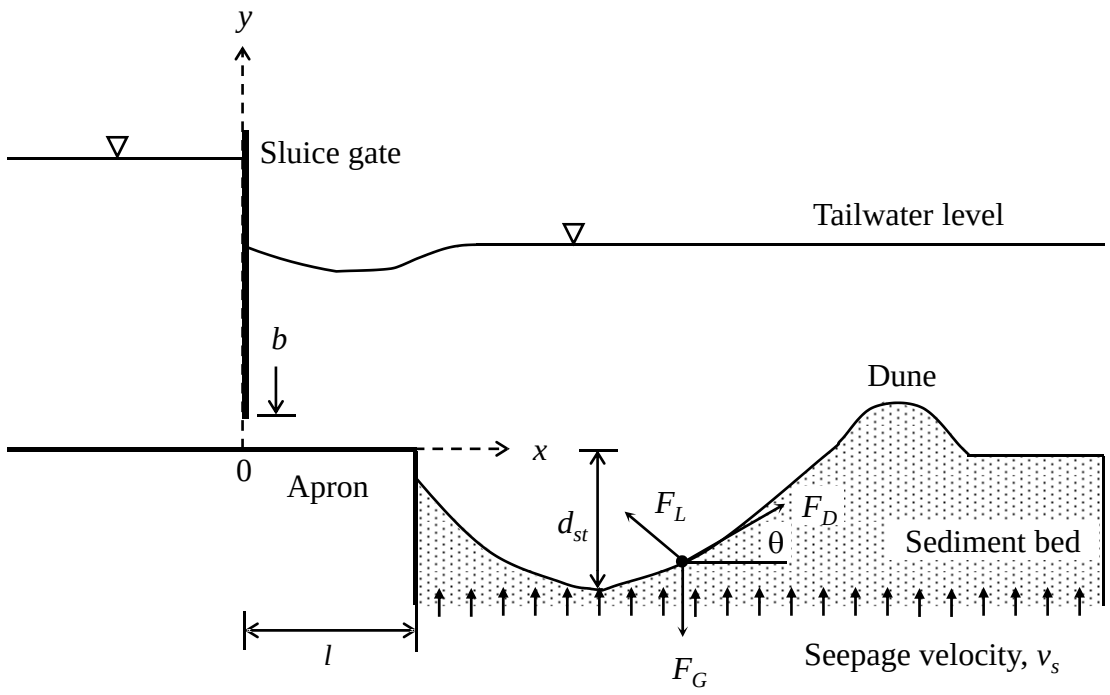

- forces acting on a sediment particle lying on the equilibrium scoured bed are the drag force F_D, lift force F_L, and submerged weight of the sediment particle F_G

- For a local streamwise bed slope θ, the threshold condition of a sediment particle can be defined by the equation proposed by Dey *et al.* (1999)

$$\tilde{\tau}_c = \cos\theta\left(1+\frac{\tan\theta}{\mu}\right) \qquad (22)$$

- $\tilde{\tau}_c$ is $[\tau_c]_{\theta=\theta}/[\tau_c]_{\theta=0}$, θ is arc tan$(d\hat{\boldsymbol{y}}/d\hat{\boldsymbol{x}})$ and μ is the Coulomb static frictional coefficient of sediment particles
- threshold shear stress for uniform sediments on a horizontal bed can be obtained from

$$\Theta(\boldsymbol{D}^* \le 1) = 0.142/\boldsymbol{D}^{*0.35}$$

$$\Theta(1 < \boldsymbol{D}^* \le 15) = 0.148/\boldsymbol{D}^{*0.36} \qquad (23)$$

$$\Theta(15 < \boldsymbol{D}^* \le 50) = 0.013\boldsymbol{D}^{*0.32}$$

$$\Theta(\boldsymbol{D}^* > 50) = 0.045$$

- $\Theta = [\tau_c]_{\theta=0}/(\Delta\rho g d_{50})$, $\Delta = s - 1$, s is the relative density of sediment particles and $D^* = d_{50}(\Delta g/\nu^2)^{1/3}$
- roughness of the loose sediment beds is defined by the median particle size d_{50}

Bed Shear Stress

- experimental values of the bed shear stress τ acting on the equilibrium scoured bed are estimated from the measured Reynolds stress profiles extending it on to the scoured bed
- nondimensional bed shear stress $[\hat{\tau}]_{\theta=\theta}$

$$[\hat{\tau}]_{\theta=\theta} = \cos\theta \; \boldsymbol{uv}^{+}\Big|_{\text{at bed}} \qquad (24)$$

- local threshold bed shear stress $[\hat{\tau}]_{\theta=\theta} = [\hat{\tau}]_{\theta=0} \cos\theta \, [1 + (\tan\theta/\mu)]$

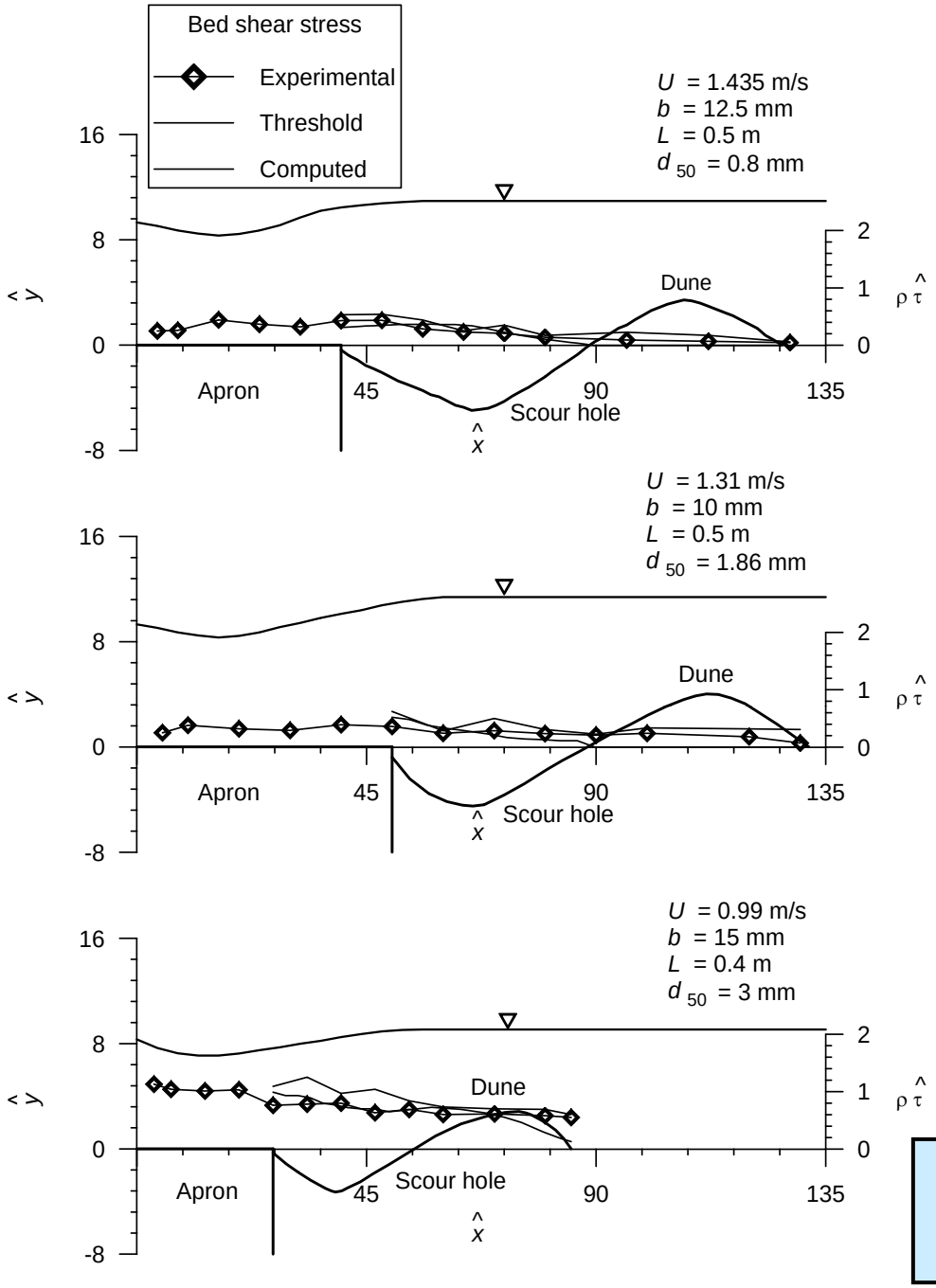

- surface of the equilibrium scour hole is at threshold condition

variations of $\rho\hat{\tau}$ on scoured beds for different runs

- assumed that the bed shear stress for the two-dimensional submerged wall jet on scoured bed is equivalent to the two-dimensional submerged wall jet on a rigid rough bed following a smooth bed
- the flow close to the bed is assumed to be not separated out from the scoured bed
- these assumptions may constitute simplifications, one can hypothesize that the bed shear stress on the equilibrium scoured bed is given by

$$[\hat{\tau}]_{\theta=\theta}(\hat{x} \geq \hat{L}) = -\Xi(\hat{x}-\hat{L},\hat{y})\left(2\hat{\delta}\hat{u}_0\frac{d\hat{u}_0}{d\hat{x}} + \hat{u}_0^2\frac{d\hat{\delta}}{d\hat{x}}\right)\int_0^{\eta}(\psi^2+\phi_1-\phi_2)d\eta$$

- function Ξ determined empirically, using the bed shear stress obtained from the measured Reynolds stress profiles within the equilibrium scour holes

$$\Xi = 0.0081\boldsymbol{c}^{4\hat{y}/\hat{\delta}} + 0.04(\boldsymbol{c}\hat{\boldsymbol{y}}/\hat{\boldsymbol{\delta}})^2 \qquad (26)$$

- parameter c in the above equation, being a function of $\hat{\boldsymbol{x}}$ and d_{50}, can be given by the following polynomial

$$\boldsymbol{c} = \boldsymbol{c}_0 + \boldsymbol{c}_1(\hat{\boldsymbol{x}} - \hat{\boldsymbol{L}}) + \boldsymbol{c}_2(\hat{\boldsymbol{x}} - \hat{\boldsymbol{L}})^2 + \boldsymbol{c}_3(\hat{\boldsymbol{x}} - \hat{\boldsymbol{L}})^3 + \boldsymbol{c}_4(\hat{\boldsymbol{x}} - \hat{\boldsymbol{L}})^4 \qquad (27)$$

- values of the coefficients c_0, c_1, c_2, c_3 and c_4 for different d_{50}

d_{50} (mm)	c_0		c_1		c_2		c_3		c_4		
	$y \le 0$	$y > 0$	$y \le 0$	$y > 0$	$y \le 0$	$y > 0$	$y \le 0$	$y > 0$	$y \le 0$	$y > 0$	n
0.8	50.4	0.91	-2.965	-0.12	0.0611	1.8×10^{-3}	-5×10^{-4}	-2×10^{-6}	1.5×10^{-6}	0	0.14
1.86	49.4	1.27	-2.965	-0.16	0.0611	2.6×10^{-3}	-5×10^{-4}	-2.8×10^{-6}	1.7×10^{-6}	0	0.15
3	50.8	1.64	-2.965	-0.2	0.0611	3.3×10^{-3}	-5×10^{-4}	-3.6×10^{-6}	1.6×10^{-6}	0	0.16

Profiles of Equilibrium Scour Hole

• threshold condition of a sediment particle resting on the surface of the scour hole

$$-\Xi(\hat{x}-\hat{L},\hat{y})\left(2\hat{\delta}\hat{u}_0\frac{d\hat{u}_0}{d\hat{x}}+\hat{u}_0^2\frac{d\hat{\delta}}{d\hat{x}}\right)\int_0^{\eta}(\psi^2+\phi_1-\phi_2)d\eta\geq[\hat{\tau}_c]_{\theta=0}\cos\theta\left(1+\frac{\tan\theta}{\mu}\right) \quad (28)$$

• for the limiting equilibrium, the above equation can be expressed as a differential equation

$$(\Omega^2-1)\frac{d\hat{y}}{d\hat{x}}=\mu\pm[\mu^2-(\Omega^2-1)(\Omega^2-\mu^2]^{0.5} \quad (29)$$

$$\Omega=-\frac{0.0081c^{4\hat{y}/\hat{\delta}}+0.04(c\hat{y}/\hat{\delta})^2}{[\hat{\tau}_c]_{\theta=0}}\left(2\hat{\delta}\hat{u}_0\frac{d\hat{u}_0}{d\hat{x}}+\hat{u}_0^2\frac{d\hat{\delta}}{d\hat{x}}\right)\int_0^{\eta}(\psi^2+\phi_1-\phi_2)d\eta \quad (30)$$

- Eq. 29 is a first-order differential equation, which can be solved numerically by the forth-order Runge-Kutta method to determine the variation of $\hat{y}$ with $\hat{x}$, that is the non-dimensional profile of equilibrium scour hole
- positive and negative signs are associated with the solution for scour hole ($\hat{y} \leq 0$) and dune ($\hat{y} > 0$) portions
- average value of μ was assumed to be 0.65
- sediments at the edge of the apron were washed out
- Eq. 29 was solved for the initial values of $\hat{x} = \hat{L}$ and $\hat{y} = 0.35$

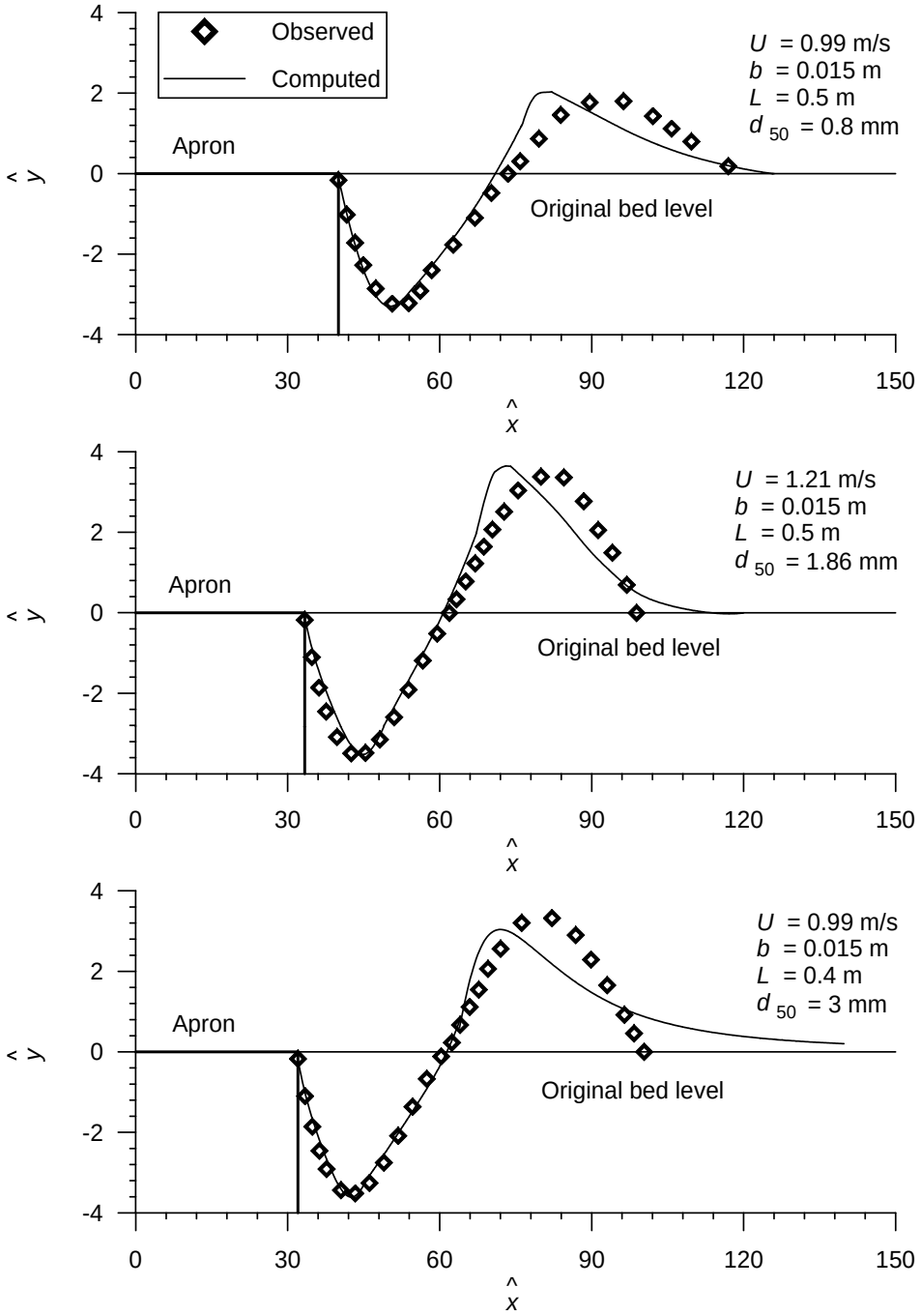

Comparisons of computed and experimental scour profiles in uniform sediments without seepage

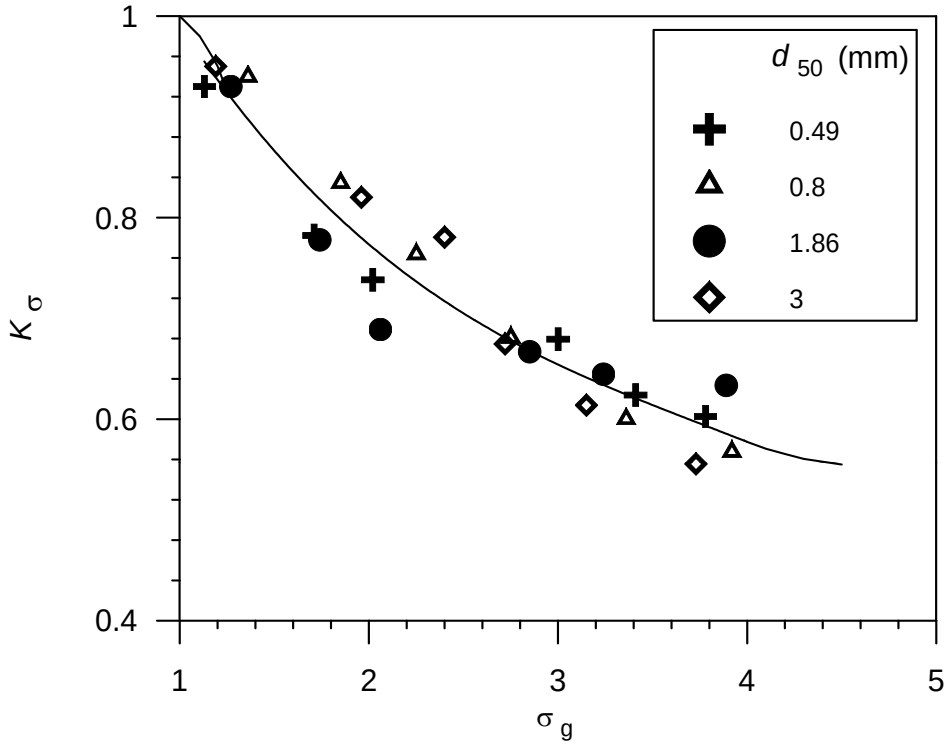

Coefficient K_σ as a function of σ_g

- particle size distribution has a pronounced influence on the scour depth
- nonuniform sediments (σ_g > 1.4) consistently produce lower scour depths than that in uniform sediments
- process of armouring in the scour hole commences resulting in an exposure of coarser particles
- armour-layer gradually increases the effective critical bed shear stress, which restricts the development of scour hole

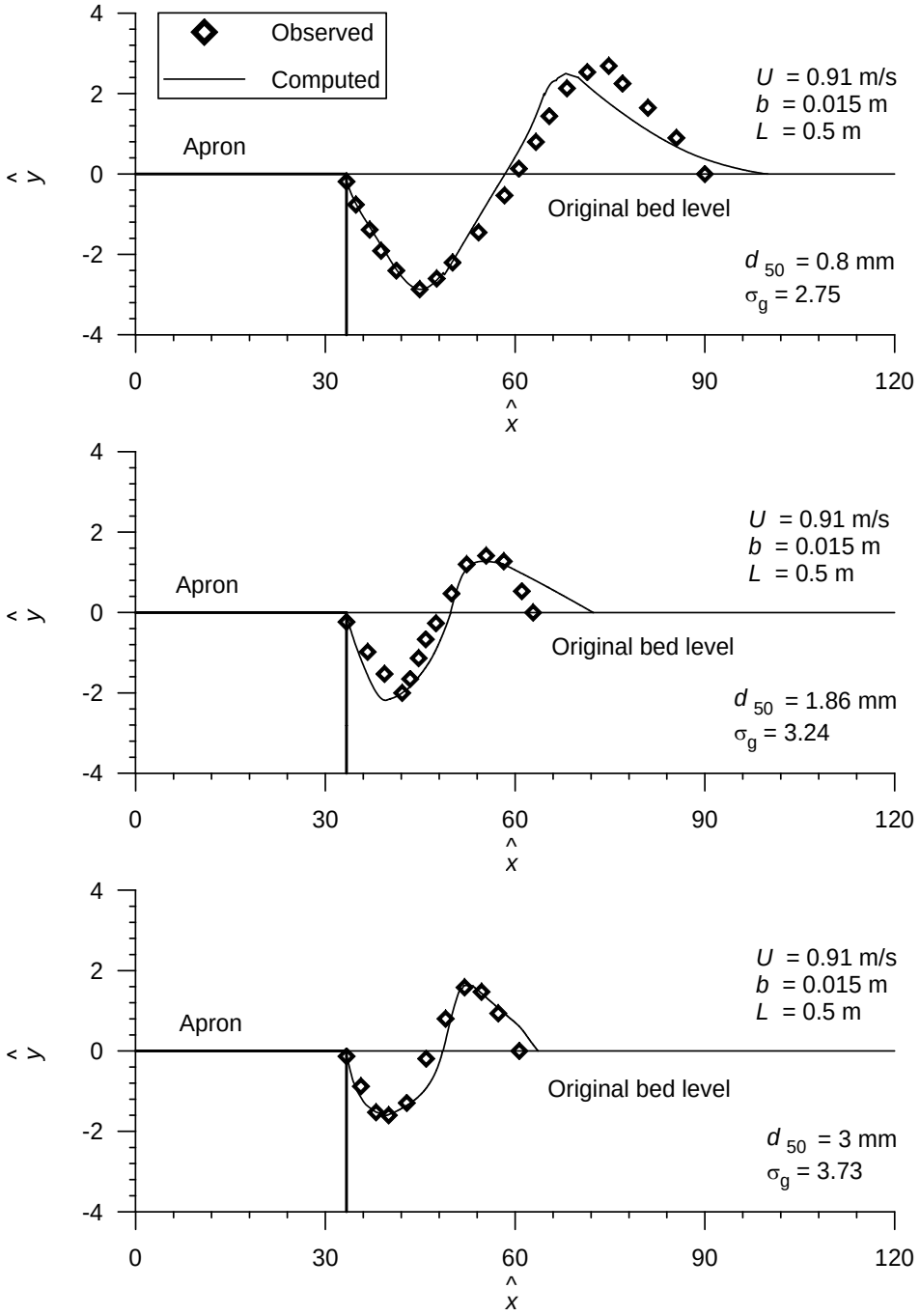

- equilibrium scour profiles can be estimated in terms of geometric standard deviation σ_g of sediments using the relationship $\hat{\boldsymbol{y}}(\sigma_g) = K_\sigma \hat{\boldsymbol{y}}$
- nonuniform sediments ($\sigma_g > 1.4$) consistently produce lower scour depths than that in uniform sediments

Comparisons of computed and experimental scour profiles in nonuniform sediments without seepage

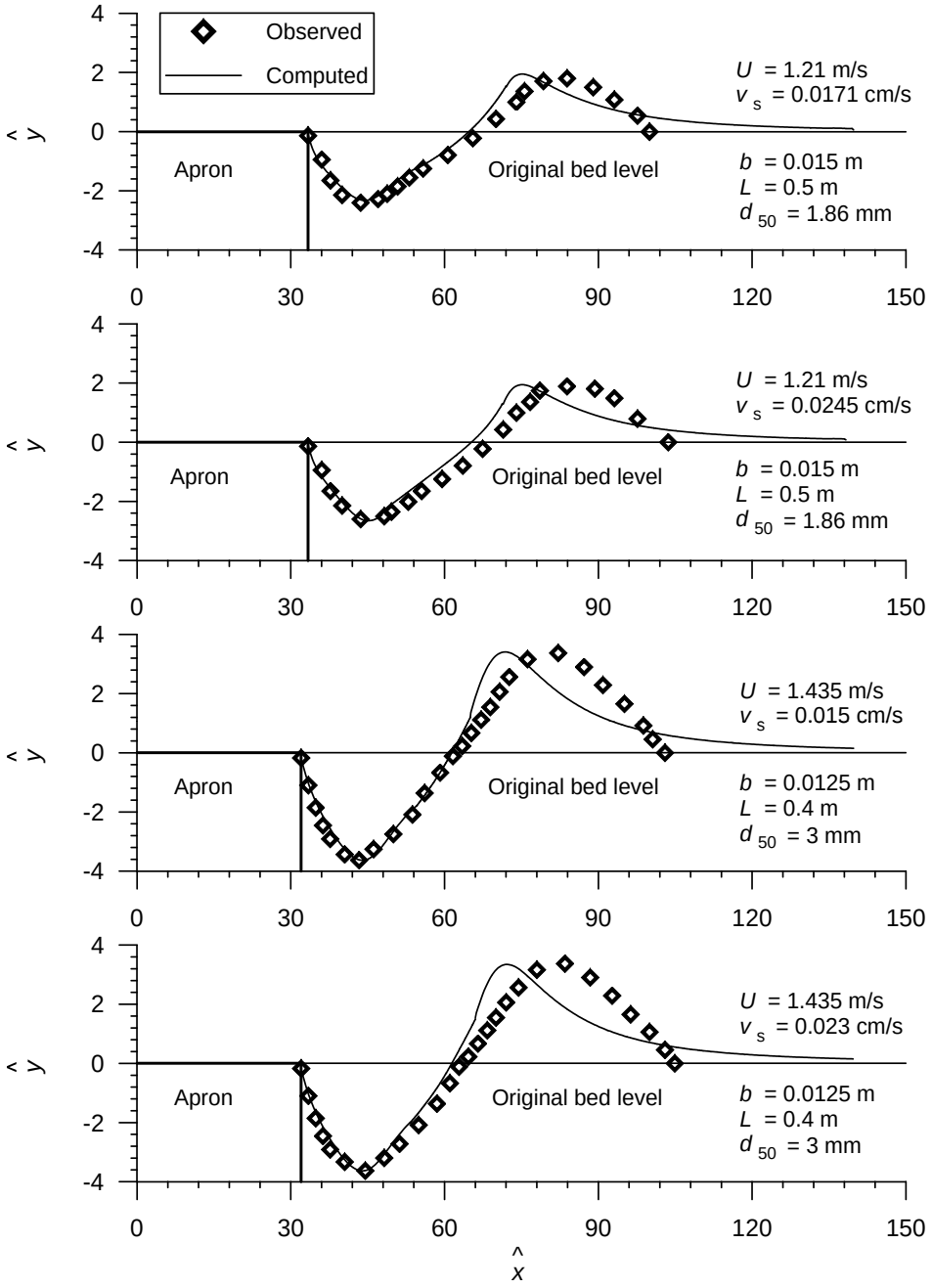

- upward seepage is a common occurrence in the sediment bed downstream of an apron due to afflux caused by the level difference of the free surface upstream the gate and the tailwater
- $[\hat{\tau}_c]_{\theta=0}$ (or Θ) is to be corrected for the upward seepage velocity v_s using the method proposed by Dey & Zanke (2004)

Comparisons of computed and experimental scour profiles in uniform sediments with seepage

- collapse of the computed and the experimentally observed profiles is good within the scour hole
- In the dune portion, the partial disagreement between the computed and the experimental profiles is due to the flow separation at the crest of the dune

Time-Variation of Maximum Scour Depth

Assumptions

- bed shear stress induced by the submerged wall jets is the main agent of scouring, picking up the sediment particles from the beds
- rate of change of sediment mass at the location (infinitesimal area) of the maximum scour depth equals the sediment mass removal rate from that location

- In small interval of time dt, sediment mass picked up from the location of maximum scour depth having small width Δx

$$dm_1 = \Delta x \, E \, dt \qquad (31)$$

E is the sediment pick-up rate at the location of the maximum scour depth at time t

• sediment pick-up rate E at location of the maximum scour depth during scouring, estimated using the equation of van Rijn (1984)

$$\boldsymbol{E} = 0.00033\rho_s(\Delta \boldsymbol{g} \boldsymbol{d}_{50})^{0.5}\, \boldsymbol{D}*^{0.3}\, \boldsymbol{T}^{1.5} \qquad (32)$$

ρ_s is the mass density of sediments and T is the transport-stage parameter due to scouring, $([\hat{\tau}]_0 - [\hat{\tau}_c]_{\theta=0})/[\hat{\tau}_c]_0$ and $[\hat{\tau}]_0$ is the bed shear stress at the location of the maximum scour depth being time dependent

• time dependent bed shear stress $[\hat{\tau}]_0$ can be hypothesized using an exponential function being dependent on d_{st}

$$[\hat{\tau}]_0 = -\exp\left[-\left(\frac{\boldsymbol{C}_0 \hat{\boldsymbol{d}}_{st}}{\hat{\boldsymbol{\delta}}}\right)^{n}\right]\left(2\hat{\delta}\hat{u}_0 \frac{d\hat{u}_0}{d\hat{x}} + \hat{u}_0^2 \frac{d\hat{\delta}}{d\hat{x}}\right)\int_0^{\eta}(\psi^2 + \phi_1 - \phi_2)\,d\eta \qquad (33)$$

• in equilibrium profiles, the average horizontal locations of maximum scour depth are approximately at $\hat{x} = \hat{L} + 10$

• using the bed shear stresses obtained from the measured Reynolds stress profiles at the locations of maximum scour depth of intermediate and equilibrium scour holes, the equations of C_0 and n are determined empirically

• equation of C_0 is given by $C_0 = 0.02 \exp(1.09F)$

• depletion of sediment mass due to an increase in scour depth dd_{st} in time dt

$$dm_2 = -(1-\rho_0)\,\rho_s\,\Delta x\,dd_{st} \qquad (34)$$

• ρ_0 is the porosity of sediments and d_{st} is the instantaneous maximum scour depth at time t, $\rho_0 = 0.4$

• Applying the conservation of the mass of sediment

$$dm_1 + dm_2 = 0 \qquad (35)$$

• Substituting Eqs. 31 and 34 in 35, differential equation of time-variation of maximum scour depth in nondimensional form

$$\frac{d\hat{d}_{st}}{d\hat{t}} = \frac{\phi_p}{(1-\rho_0)\hat{d}} \qquad (36)$$

• $\hat{d}_{st}$ is d_{st}/b, $\hat{t}$ is the time parameter, that is $td_{50}(\Delta g d_{50})^{0.5}/b^2$, ϕ_p is the sediment pickup function, that is $E/[\rho_s(\Delta g d_{50})^{0.5}]$ and $\hat{d}$ is d_{50}/b

- Eq. 36 is solved numerically to determine the variation of $\hat{d}_{st}$ with $\hat{t}$ for a given issuing jet velocity, sluice opening, apron length and sediment size
- in nonuniform sediments, values of $\hat{d}_{st}$ obtained from (7.15) have to be multiplied by the coefficient K_σ for the sediment gradation σ_g
- to determine the scour profiles under upward seepage, $[\hat{\tau}_c]_{\theta=0}$ (or Θ) is to be corrected for the upward seepage velocity v_s using the method proposed by Dey & Zanke (2004)

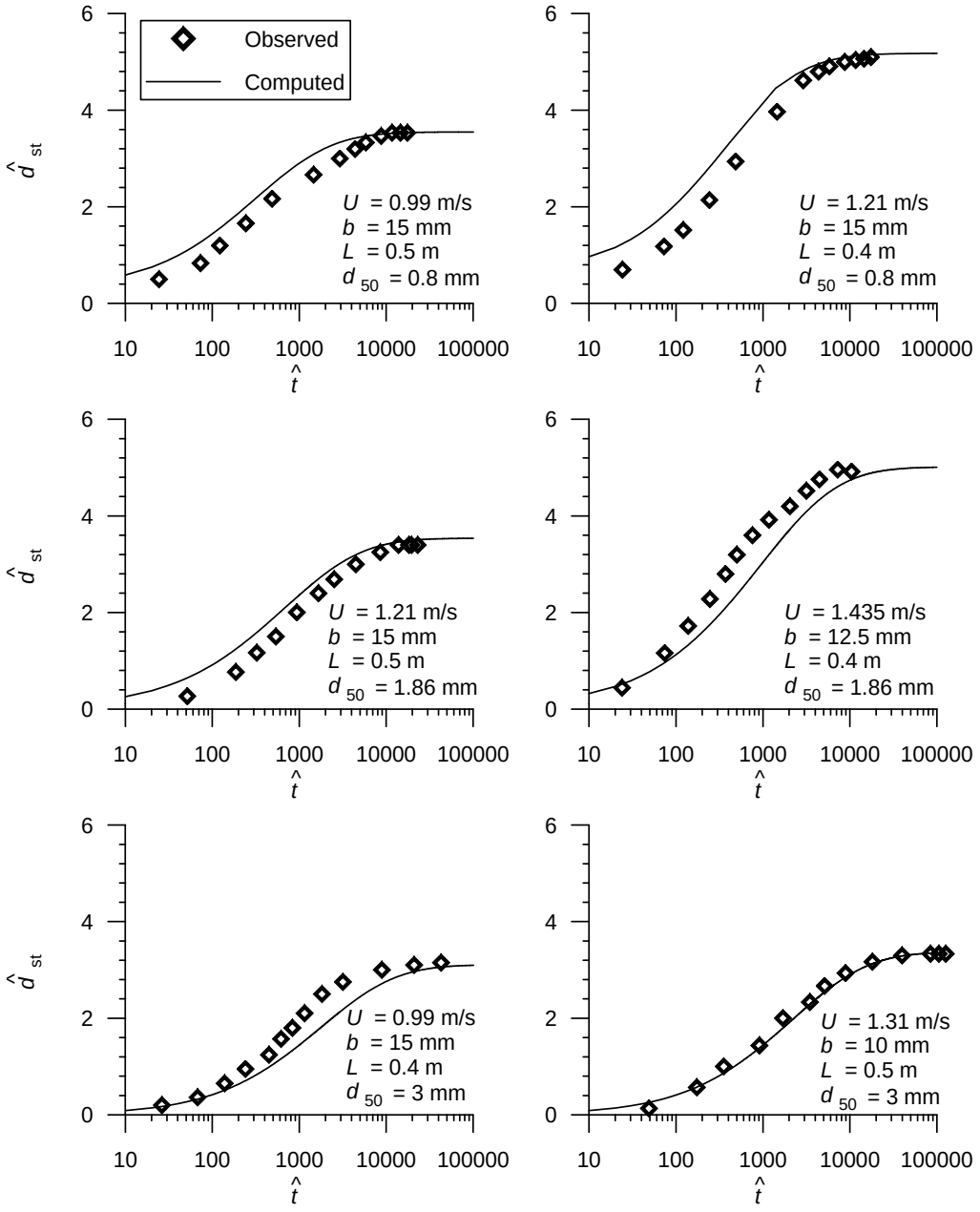

Comparisons of computed and experimental time-variation of scour depth in uniform sediments without seepage

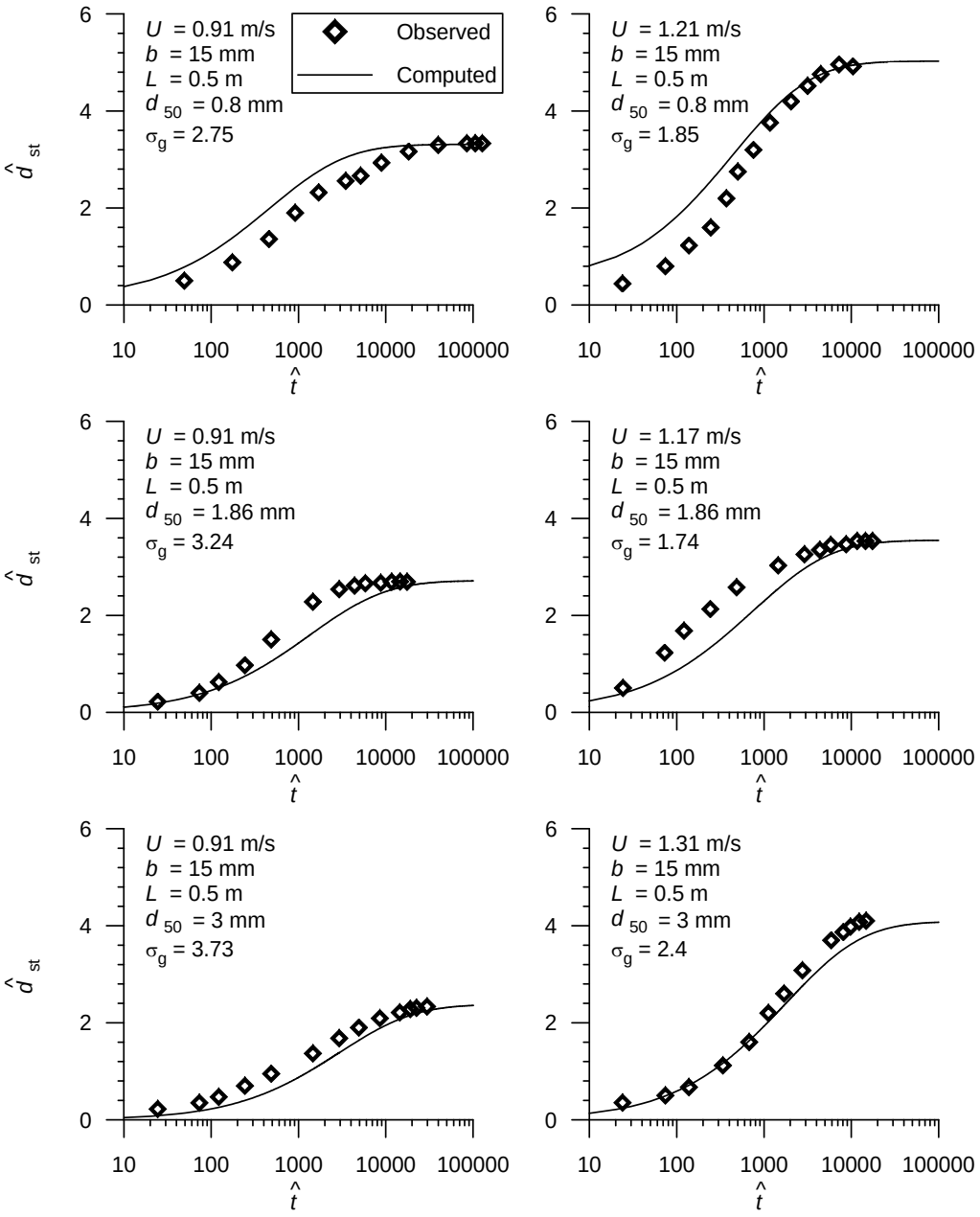

Comparisons of computed and experimental time-variation of scour depth in nonuniform sediments without seepage

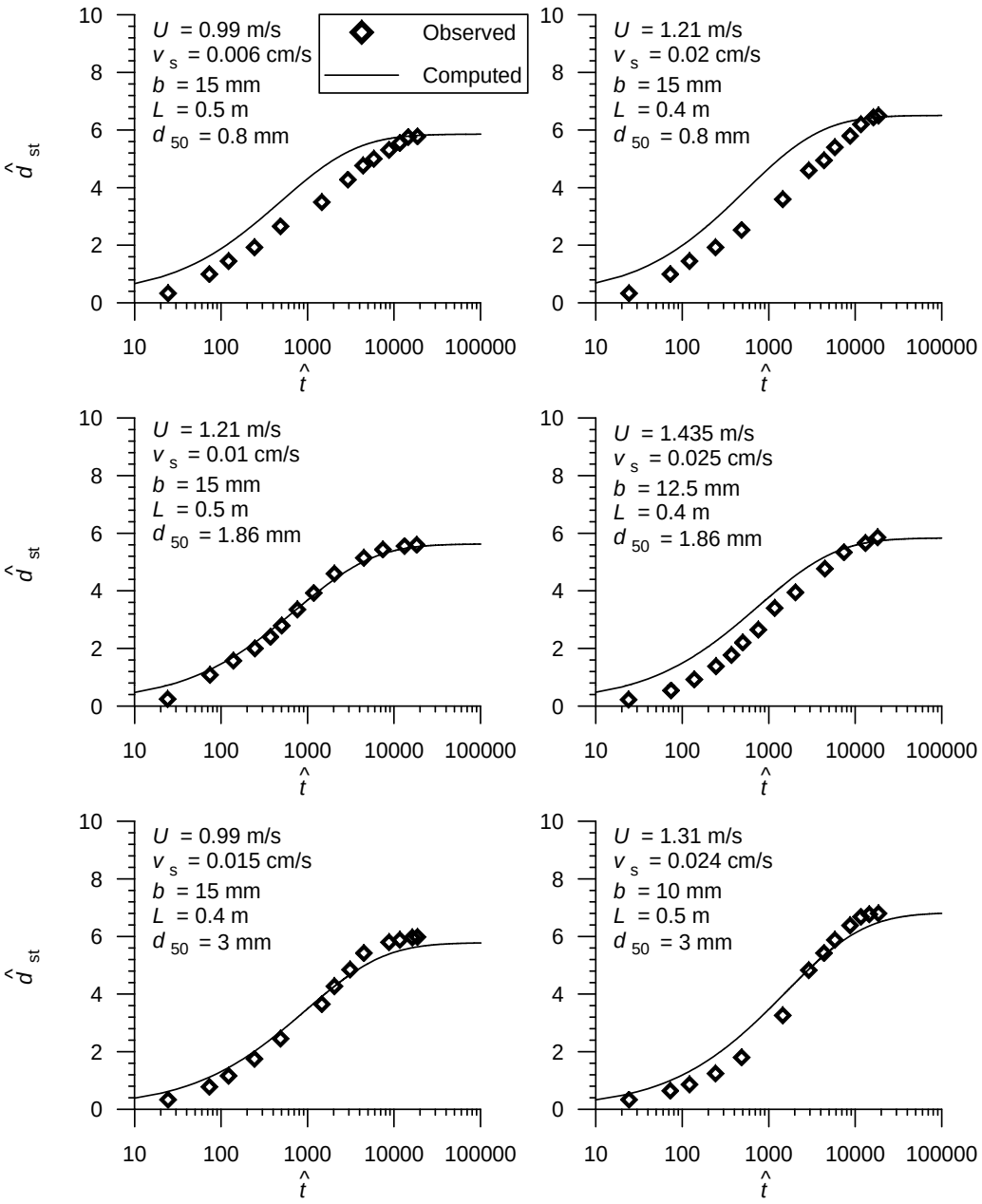

Comparisons of computed and experimental time-variation of scour depth in uniform sediments with seepage

Thank You